AD-A229 779

DTIC ACCESSION NUMBER

PHOTOGRAPH THIS SHEET

LEVEL

INVENTORY 1

AFWAL-TR-87-4117

DOCUMENT IDENTIFICATION

MAR 1987

DISTRIBUTION STATEMENT A

Approved for public release;
Distribution Unlimited

DISTRIBUTION STATEMENT

ACCESSION FOR

NTIS GRA&I X

DTIC TRAC ☐

UNANNOUNCED ☐

JUSTIFICATION

BY

DISTRIBUTION/

AVAILABILITY CODES

DISTRIBUTION	AVAILABILITY AND/OR SPECIAL	
A-1		

DISTRIBUTION STAMP

DTIC
ELECTE
JAN 03 1991
D

DATE ACCESSIONED

DATE RETURNED

91 1 2 00

DATE RECEIVED IN DTIC

REGISTERED OR CERTIFIED NUMBER

PHOTOGRAPH THIS SHEET AND RETURN TO DTIC-FDAC

DTIC FORM 70A APR 87

DOCUMENT PROCESSING SHEET

PREVIOUS EDITIONS MAY BE USED UNTIL STOCK IS EXHAUSTED

AFWAL-TR-87-4117

INITIAL IMPACT DAMAGE OF COMPOSITES

Jonathan Goering, B. Walter Rosen, Brian Coffenberry
Materials Sciences Corporation
Gwynedd Plaza II
Bethlehem Pike
Spring House PA 19477

March 1987

Final Report for Period November 1985 - February 1987

MATERIALS LABORATORY
AIR FORCE WRIGHT AERONAUTICAL LABORATORIES
AIR FORCE SYSTEMS COMMAND
WRIGHT-PATTERSON AIR FORCE BASE, OHIO 45433-6533

NOTICE

When government drawings, specifications, or other data are used for any purpose other than in connection with a definitely related government procurement operation, the United States government thereby incurs no responsibility nor any obligation whatsoever; and the fact that the government may have formulated, furnished, or in any way supplied the said drawings, specifications, or other data, is not to be regarded by implication or otherwise as in any manner licensing the holder or any other person or corporation, or conveying any rights or permission to manufacture, use, or sell any patented invention that may in any way be related thereto.

This report has been reviewed by the Office of Public Affairs (ASD/PA) and is releasable to the National Technical Information Service (NTIS). At NTIS, it will be available to the general public, including foreign nations.

This technical report has been reviewed and is approved for publication.

JAMES M. WHITNEY, Project Engineer
Mechanics & Surface Interactions Br
Nonmetallic Materials Division

FOR THE COMMANDER

MERRILL L. MINGES, SES, Director
Nonmetallic Materials Division

If your address has changed, if you wish to be removed from our mailing list, or if the addressee is no longer employed by your organization, please notify AFWAL/MLBM Wright-Patterson AFB, OH 45433-6533 to help us maintain a current mailing list.

Copies of this report should not be returned unless return is required by security considerations, contractual obligations, or notice on a specific document.

REPORT DOCUMENTATION PAGE

Form Approved OMB No. 0704-0188

1a. REPORT SECURITY CLASSIFICATION: Unclassified	1b. RESTRICTIVE MARKINGS
2a. SECURITY CLASSIFICATION AUTHORITY	3. DISTRIBUTION/AVAILABILITY OF REPORT: Approved for public release; distribution is unlimited.
2b. DECLASSIFICATION/DOWNGRADING SCHEDULE	
4. PERFORMING ORGANIZATION REPORT NUMBER(S)	5. MONITORING ORGANIZATION REPORT NUMBER(S): AFWAL-TR-87-4117
6a. NAME OF PERFORMING ORGANIZATION: Materials Sciences Corporation; 6b. OFFICE SYMBOL (If applicable): N/A	7a. NAME OF MONITORING ORGANIZATION: Air Force Wright Aeronautical Laboratories Materials Laboratory (AFWAL/MLBM)
6c. ADDRESS (City, State, and ZIP Code): Gwynedd Plaza II, Bethlehem Pike, Spring House PA 19477	7b. ADDRESS (City, State, and ZIP Code): Wright-Patterson AFB OH 45433-6533
8a. NAME OF FUNDING/SPONSORING ORGANIZATION; 8b. OFFICE SYMBOL (If applicable)	9. PROCUREMENT INSTRUMENT IDENTIFICATION NUMBER: F33615-85-C-5156
8c. ADDRESS (City, State, and ZIP Code)	10. SOURCE OF FUNDING NUMBERS: PROGRAM ELEMENT NO. 65502F; PROJECT NO. 3005; TASK NO. 50; WORK UNIT ACCESSION NO. 61

11. TITLE (Include Security Classification): Initial Impact Damage of Composites

12. PERSONAL AUTHOR(S): Jonathan Goering; B. Walter Rosen; Brian Coffenberry

13a. TYPE OF REPORT	13b. TIME COVERED	14. DATE OF REPORT (Year, Month, Day)	15. PAGE COUNT
Final Report	FROM 11/85 TO 02/87	January 1988	95

16. SUPPLEMENTARY NOTATION

17. COSATI CODES			18. SUBJECT TERMS (Continue on reverse if necessary and identify by block number)
FIELD	GROUP	SUB-GROUP	Composite, Impact, Laminate Analysis, Dynamic Loading
13	13		

19. ABSTRACT (Continue on reverse if necessary and identify by block number)

An analytical model is developed for predicting and studying the transient dynamic response of laminated composites during impact loading. In order to determine local stresses, the laminate is modeled as a number of substructures, each of which is representative of a smaller portion of the laminate. The reduced substructures are assembled in a manner analogous to classical finite elements. Good agreement was found between experimental and analytical contact force histories for 16 ply graphite/epoxy plates with aspect ratios less than 4.0. Less agreement was obtained for aspect ratios above 40.

20. DISTRIBUTION/AVAILABILITY OF ABSTRACT: ☒ UNCLASSIFIED/UNLIMITED ☐ SAME AS RPT. ☐ DTIC USERS	21. ABSTRACT SECURITY CLASSIFICATION: Unclassified
22a. NAME OF RESPONSIBLE INDIVIDUAL: J. Whitney	22b. TELEPHONE (Include Area Code): (513) 255-9097; 22c. OFFICE SYMBOL: AFWAL/MLBM

PREFACE

This report summarizes the work performed for the Air Force Wright Aeronautical Laboratories (AFWAL) under Contract F33615-85-C-5156, Project 3005, during the period of November 15, 1985 to February 15, 1987. Mr. Jonathan Goering was the principal investigator for Materials Sciences Corporation (MSC). Dr. B. Walter Rosen served as the program manager, and Mr. Brian Coffenberry assisted in performing the impact analyses. The AFWAL technical monitor for this program was Dr. J. M. Whitney.

TABLE OF CONTENTS

Section		Page
I.	INTRODUCTION	1
II.	ANALYTICAL MODEL	2
	1. OVERVIEW	2
	2. LAMINATED SOLID FINITE ELEMENTS	4
	3. NON-LINEAR CONTACT MODEL	13
	4. EQUATIONS OF MOTION	14
	5. FAILURE ANALYSIS	18
III.	ANALYSIS	21
	1. MODEL DESCRIPTIONS	21
	2. RESULTS	22
IV.	DISCUSSION AND CONCLUSIONS	26
	REFERENCES	32
	APPENDIX - SOFTWARE DESCRIPTION	66

LIST OF TABLES

Tables		Page
1.	AS4/3502 Analysis Summary	34
2.	Material Properties for AS4/3502 Analyses	35
3.	Contact Law Parameters for AS4/3502 Analyses	36
4.	IM6/934 Analysis Summary	37
5.	Aspect Ratio Summary	38
6.	Generalized Coordinate Analysis Summary (IM6/934)	39

LIST OF ILLUSTRATIONS

Figures		Page
1.	Experimental Contact Force History Comparison for 8 Ply Laminates with 75 mm Diameter Support	40
2.	Experimental Contact Force History Comparison for 16 Ply Laminates with 75 mm Diameter Support	41
3.	Model Building Sequence	42
4.	2-D Element Nomenclature	43
5.	Special 3-D Geometry	44
6.	General 3-D Geometry	45
7.	Local Coordinate Mapping	46
8.	Typical Force-Deflection Diagram for the Contact Spring	47
9.	AS4/3502 1/4 Plate Model	48
10.	IM6/934 1/4 Plate Model	49
11.	Impactor and Impacted Node Displacement Histories for 16 Ply AS4/3502 Laminate with 50 mm Diameter Support	50
12.	Contact Force History Comparison for 16 Ply AS4/3502 Laminate with 50 mm Diameter Support	51
13.	Normalized Stress Histories for 16 Ply AS4/3502 Laminate with 50 mm Diameter Support	52

LIST OF ILLUSTRATIONS, (Cont'd)

Figure		Page
14.	Contact Force History for IM6/934 Laminate Impact Energy = 1.92 N-m	53
15.	Contact Force History for 16 Ply AS4/3502 Laminate with 75 mm Diameter Support	54
16.	Contact Force History for 8 Ply AS4/3502 Laminate with 25 mm Diameter Support	55
17.	Contact Force History for 8 Ply AS4/3502 Laminate with 50 mm Diameter Support	56
18.	Contact Force History for 8 Ply AS4/3502 Laminate with 75 mm Diameter Support	57
19.	Extensional Strain Comparison for 8 Ply AS4/3502 Laminate with 50 mm Diameter Support	58
20.	Generalized Coordinates for IM6/934 Laminate with Large Mass Impactor. Impact Energy = 3.84 N-m	59
21.	Generalized Coordinates for IM6/934 Laminate with Small Mass Impactor. Impact Energy = 3.84 N-m	60
A-1.	2-D Element Description	A-4
A-2.	3-D Rectangular Element Description	A-5
A-3.	3-D General Element Description	A-6

I. INTRODUCTION

The damaging effect of low velocity impact upon laminated composite structures has been recognized by the engineering community as an area of primary concern. This type of loading can easily be envisioned as a workmans tool being dropped on a structure during assembly, or runway debris thrown against a composite airframe during takeoff or landing. The damage produced by these loads may consist of matrix cracking, delaminations and even fiber failures, depending on the mass and velocity of the impactor. Often, this damage is invisible to the naked eye, and may go unnoticed even though the strength of the structure has been seriously degraded.

The primary objective of Phase I of this program was the development of an analytical model for studying the transient dynamic response of laminated composites during this type of impact event. This model utilized a plate bending finite element to characterize the laminate and a lumped mass and nonlinear contact force spring to characterize the impactor. The discretized equations of motion were generated, and integrated numerically to yield the displacement history of the system. The displacement history could then be used to determine the strain, and ultimately stress histories for the laminate. These stresses and/or strains were then used to predict the onset of damage in the plate (Ref. 1).

The Phase I model predicts stresses and strains which are consistent with the plate bending assumptions. That is, extensional strains vary linearly through-the-thickness of the plate, and shear strains vary parabolically. The distributions predicted by the model are then a good representation of the far field solution, but do not adequately describe the complex fields that may exist in close proximity to the impactor.

Accurate characterization of these stress and strain fields is important since they may result in peak values and distributions that are substantially different from those predicted by plate bending theory. Development of a more refined model for predicting the three-dimensional state of stress in the vicinity of the impactor has been the focus of the Phase II work.

This work has concentrated on three topics; development of a three-dimensional laminated solid finite element, optimization of the algorithms used to generate and solve the equations of motion, and validation of the resulting analytical model.

II. ANALYTICAL MODEL

1. OVERVIEW

The intent of the analytical model is to provide an accurate tool for predicting the initiation of damage in a laminated composite due to low-velocity impact. The definition of low-velocity impact is debatable, but for this program it will be interpreted as an impact event which produces dynamic effects that are dominated by flexural waves.

To allow generality in defining parameters such as plate geometry and boundary conditions, finite elements are used to model the laminate. The impactor is assumed to be very stiff relative to the plate allowing it to be treated as a lumped mass coupled to the plate through some suitable contact law.

It was assumed that all material non-linearities would only be apparent in a localized region near the impact site, and could be incorporated into the contact model rather than the stiffness of the laminate. This allows the initial stiffness of the laminate to be used throughout the analysis. This assumption is validated to some extent by experiments performed by AFML on plates with either epoxy or thermoplastic matrices.

Figures 1 and 2 show the experimental responses of graphite/epoxy and graphite/PEEK plates to the same impact event. Figure 1 shows the contact force history for 8 ply laminates simply supported over a 50 mm diameter circle, and Figure 2 shows the same for 16 ply laminates. The two matrix systems used in these plates have essentially the same initial stiffness, but the thermoplastic is much more ductile. The figures show that the response of the two material systems are similar up to the initiation of damage, which is consistent with the assumption stated above. It is further assumed that differences in the point at which damage occurs may be attributed to differences in the strength of the two matrices, rather than differences in the dynamic response.

Objectives of the impact analysis are to predict both an accurate flexural response and an accurate stress distribution. The level of refinement needed to predict accurate stresses in a finite element model is typically much greater than the refinement necessary for accurate

displacements. This results in a dynamic model which includes for more degrees of freedom than are necessary for predicting displacement histories.

To overcome this problem, the laminate is modeled as a number of substructures, each of which is representative of a smaller portion of the complete laminate. A reduction procedure is used which defines the effective mass and stiffness of the substructure in terms of a small number of "master" degrees of freedom. The response of the complete substructure may then be approximated, given the response of the master degrees of freedom.

The reduced substructures are then assembled, similar to the assembly of typical finite elements, into a model of the complete laminate. The same type of reduction is then performed on the full model, allowing the response of the complete set of master degrees of freedom to be approximated by the response of a set of "governor" degrees of freedom.

Adding the contact model to the reduced dynamic model of the laminate then gives the reduced equations of motion for the plate/impactor system. These equations are integrated to give the response of the governor degrees of freedom. This response is expanded to give the response of all master degrees of freedom, which are then used to give the complete displacement response of each substructure. This model building sequence is shown schematically in Figure 3.

For a given substructure, the displacement solution at a point in time is used to calculate strains. From this strain distribution stresses are calculated and used in a suitable failure criteria to assess failure in that substructure at that time. These calculations are performed for each substructure at regular time intervals to predict the onset of damage.

The analytical procedure then consists of three phases: substructure generation and reduction; global model assembly, reduction, and solution; and back substitution, stress and failure analysis. Since the mass and stiffness of the laminate are assumed to be constant, the model generation, assembly and reduction can be performed once and used throughout the analysis.

2. LAMINATED SOLID FINITE ELEMENTS

A number of displacement shape functions were considered for use in this program. Two-dimensional elements were developed with these shape functions and used to evaluate the relative merits of the functions. An element's ability to approximate the complex stress distributions through the thickness of a short beam in three point bending was used as a benchmark.

From these analyses, it was determined that the most appropriate element for further development was a subparametric element which utilized cubic displacement shape functions, and included first derivatives of displacements as nodal variables. The details and findings of this study have been documented in Reference 2.

Cubic shape functions are particularly well suited for modeling beams and plates since the classical beam and plate theories assume cubic displacement fields. Shear strain distributions in this element are then quadratic, allowing a parabolic distribution to be modeled with a single element through the thickness. More complex distributions are approximated with only a few elements through the thickness.

The inclusion of derivatives as nodal variables is also attractive in that it allows boundary conditions to be defined in terms of strain. For example, these derivatives may be used in conjunction with the constitutive law for a surface ply to inforce stress boundary conditions at the top and bottom surfaces of a laminate.

A two-dimensional element was developed for modeling beams, and three-dimensional elements were developed for modeling plates. Both types of elements were incorporated into computer programs which generate and reduce beam or plate substructures, as previously described. Descriptions of these programs are included in the Appendix.

2-D Element

The two-dimensional element is based upon the work of Webster (3), extended to account for step changes in material properties through the thickness of the element. This extension allows a single element to model several plies in a laminate.

A subparametric formulation is used, in which the element geometry is restricted to be a unit width rectangle, with sides parallel to the global axes. The 2-D geometry and nomenclature are shown in Figure 4. Geometric shape functions for the elements are given by

$$g(x,z) = \sum_{i=1}^{4} N_i g_i \qquad (1)$$

where

$$g_i = g(x_i, z_i)$$

$$N_i = \frac{1}{4}(1+x_o)(1+z_o)$$

and

$$x_o = xx_i$$

$$z_o = zz_i$$

where (x_i, z_i) are the local coordinates of node i.

Nodal variables for the element consist of translations in the x and z directions (u and w), and the first derivatives of these displacements with respect to x and z ($u_{,x}$, $u_{,z}$, $w_{,x}$, and $w_{,z}$). The displacement shape function is

$$f(x,z) = \sum_{i=1}^{4} [N]_i (f_i) \qquad (2)$$

where

$$(f)_i^T = (f_i \quad f_{,x_i} \quad f_{,z_i})$$

$$[N]_i = [N_i \quad N_{x_i} \quad N_{z_i}]$$

and the components of $[N]_i$ are given by

$$N_i = \frac{1}{8}(1+x_o)(1+z_o)(2+x_o(1-x_o) + z_o(1-z_o)) \tag{3a}$$

$$N_{x_i} = -\frac{1}{8}(1+x_o)^2(1+z_o)(1-x_o)x_i \tag{3b}$$

$$N_{z_i} = -\frac{1}{8}(1+x_o)(1+z_o)^2(1-z_o)z_i \tag{3c}$$

Strain components which contribute to the strain energy in the element are the extensional strains ϵ_x and ϵ_z, and the shear strain γ_{zx}. These strains are given in terms of the displacements as

$$\{\epsilon\} = \begin{Bmatrix} \epsilon_x \\ \epsilon_z \\ \gamma_{zx} \end{Bmatrix} = \begin{Bmatrix} \frac{\partial u}{\partial x} \\ \frac{\partial w}{\partial z} \\ \frac{\partial w}{\partial x} + \frac{\partial u}{\partial z} \end{Bmatrix} \tag{4}$$

Using the shape function given by (2), the strain in the element may be expressed in terms of the nodal variables

$$\{\epsilon\} = \sum_{i=1}^{4} [B]_i \{u\}_i = [B]\{u\} \tag{5}$$

where

$$\{u\}_i^T = \{u_i \quad u_{,x_i} \quad u_{,z_i} \quad w_i \quad w_{,x_i} \quad w_{,z_i}\}$$

and

$$[B]_i = \begin{bmatrix} \frac{\partial}{\partial x}[N]_i & 0 \\ 0 & \frac{\partial}{\partial z}[N]_i \\ \frac{\partial}{\partial z}[N]_i & \frac{\partial}{\partial x}[N]_i \end{bmatrix}$$

The stress in the element is given by

$$\{\sigma\} = \begin{Bmatrix} \sigma_x \\ \sigma_z \\ \tau_{zx} \end{Bmatrix} = [C]\{\epsilon\} \tag{6}$$

where [C] is the constitutive law that has been modified to reflect a state of either plane stress or plane strain. Using (5), the stress may be expressed in terms of the nodal variables as

$$\{\sigma\} = [C][B]\{u\} \tag{7}$$

Using (5) and (7), the stiffness of the element may be found by minimizing potential energy, yielding

$$[K_e] = \int^V [B]^T[C][B]dv \tag{8}$$

Since the material properties in a laminate are piecewise constant through the thickness, the integral in (8) may be expressed as

$$[K_e] = \sum_{i=1}^{n} \int_{-\ell/2}^{\ell/2} \int_{z_i^-}^{z_i^+} [B]^T[C]_i[B]\, dzdx \tag{9}$$

where z_i^+ and z_i^- are the locations of the top and bottom surfaces of the ith ply respectively, and $[C]_i$ is the constitutive law for the ith ply.

A consistant mass matrix is generated for the element, using the geometric shape function given by (1). This matrix is evaluated using the integral

$$[M_e] = \int^V [N']^T\rho[N']dv \tag{10}$$

As with the constitutive law, the density of the laminate is piecewise constant through the thickness. The mass matrix may then be evaluated by

$$[M_e] = \sum_{i=1}^{n} \int_{-\ell/2}^{\ell/2} \int_{z_i^-}^{z_i^+} [N']^T \rho_i [N'] dz dx \tag{11}$$

where ρ_i is the density of the ith ply.

This mass matrix only associates inertia with translational degrees of freedom. However, since there is a mass distribution through the thickness, an inertial effect analogous to rotary inertia is included.

When a displacement solution has been found, the strain at a point in the element may be evaluated using (5). The stress corresponding to this strain is then given by (6). Average strain in a ply may be found by integrating (5) over the volume of that ply contained in the element. This average strain is given by

$$\{\bar{\epsilon}\}_i = \left(\frac{1}{V_i} \int_{\ell/2}^{\ell/2} \int_{z_i^-}^{z_i^+} [B] dz dx\right)\{u\} \tag{12}$$

where V_i is the volume of ply i contained in the element. The average stress in the ply is then given by

$$\{\bar{\sigma}\}_i = [C]_i \{\bar{\epsilon}\}_i \tag{13}$$

A similar procedure may be performed to determine the average states of stress and strain at a ply interface. It is assumed that the interface has no thickness, allowing the integration to be performed over the interface area, rather than volume. Using (5), the average strain at an interface is

$$\{\bar{\epsilon}\}_j = \left(\frac{1}{A_j} \int_{-\ell/2}^{\ell/2} [B(x,z_j)] dx\right)\{u\} \tag{14}$$

where A_j is the surface area of the jth interface contained in the element.

The average stress at the interface is then

$$\{\bar{\sigma}\}_j = [C]_j \{\bar{\epsilon}\}_j \tag{15}$$

where $[C]_j$ is the constitutive law for the interface. Note that since the volume of the interface is zero, it does not contribute to the mass or stiffness of the element.

3-D Elements

Two three-dimensional elements were developed, both of which utilize cubic displacement functions and retain first derivatives as nodal degrees of freedom. The first of these is an extension of the two-dimensional element, and requires that the element geometry be a rectangular hexadedron with sides parallel to the global coordinate axes (Figure 5). The second element is less restrictive in that it allows the geometry to be a uniform thickness prism, defined by an arbitrary quadrilateral in the x-y plane (Figure 6). Since the rectangular element is a special case of the prismatic element, the formulation of the general geometry will be given first, and degenerated for the special case.

Formulation of the element is simplified by mapping the element geometry onto a two unit cube as shown in Figure 7. Edges of the element are restricted to be straight lines, allowing a subparametric formulation. In the local (r,s,q) coordinate system, the geometric shape function is given by

$$g(r,s,q) = \sum_{i=1}^{8} N_i' \, g_i \qquad (16)$$

where

$$g_i = g(r_i, s_i, q_i)$$

$$N_i' = \frac{1}{8}(1+r_o)(1+s_o)(1+q_o)$$

and

$$r_o = rr_i$$

$$s_o = ss_i$$

$$q_o = qq_i$$

where (r_i, s_i, q_i) are the coordinates of node i in the local coordinate system.

Nodal variables for this element consist of translations in each coordinate direction (u,v and w), and the first derivatives of these translations with respect to each coordinate. Displacement shape functions are cubic polynomials in the local coordinate system, given by

$$f(r,s,t) = c_o + c_1 r + c_2 s + c_3 q + c_4 r^2 + c_5 rs + c_6 s^2 + c_7 sq + c_8 q^2 \qquad (17)$$
$$+ c_9 qr + c_{10} r^3 + c_{11} r^2 s + c_{12} rs^2 + c_{13} s^3 + c_{14} s^2 q + c_{15} sq^2$$
$$+ c_{16} q^3 + c_{17} q^2 r + c_{18} qr^2 + c_{19} rsq + c_{20} r^3 s + c_{21} rs^3 + c_{22} s^3 q$$
$$+ c_{23} sq^3 + c_{24} q^3 r + c_{25} qr^3 + c_{26} r^2 sq + c_{27} rs^2 q + c_{28} rsq^2$$
$$+ c_{29} r^3 sq + c_{30} rs^3 q + c_{31} rsq^3$$

Expressed in terms of the local nodal variables, the displacement shape functions are

$$f(r,s,q) = \sum_{i=1}^{8} [N]_i (f')_i \qquad (18)$$

where

$$(f')_i^T = (f_i \quad f_{,r_i} \quad f_{,s_i} \quad f_{,t_i})$$

and

$$[N]_i = [N_i \quad N_{r_i} \quad N_{s_i} \quad N_{q_i}]$$

where the components of $[N]_i$ are given by

$$N_i = \frac{1}{16}(1+r_o)(1+s_o)(1+q_o)(2+r_o(1-r_o) + s_o(1-s_o) + q_o(1-q_o)) \qquad (19a)$$

$$N_{r_i} = -\frac{1}{16}(1+r_o)^2(1+s_o)(1+q_o)(1-r_o)r_i \qquad (19b)$$

$$N_{s_i} = -\frac{1}{16}(1+r_o)(1+s_o)^2(1+q_o)(1-s_o)s_i \tag{19c}$$

$$N_{q_i} = -\frac{1}{16}(1+r_o)(1+s_o)(1+q_o)^2(1-q_o)t_i \tag{19d}$$

The nodal derivatives used in (18) are taken with respect to the local coordinates, and must be transformed into the global coordinate system. Using the geometrical shape functions given in (16), and the chain rule, the transformation from global to local variables is given by

$$(f')_i = [J']_i(f)_i \tag{20}$$

where

$$(f)_i^T = (f_i \quad f_{,x_i} \quad f_{,y_i} \quad f_{,z_i})$$

and

$$[J'] = \begin{bmatrix} 1 & 0 & 0 & 0 \\ 0 & \sum_{j=1}^{8} \frac{\partial N_j'}{\partial r} x_j & \sum_{j=1}^{8} \frac{\partial N_j'}{\partial r} y_j & \sum_{j=1}^{8} \frac{\partial N_j'}{\partial r} z_j \\ 0 & \sum_{j=1}^{8} \frac{\partial N_j'}{\partial s} x_j & \sum_{j=1}^{8} \frac{\partial N_j'}{\partial s} y_j & \sum_{j=1}^{8} \frac{\partial N_j'}{\partial s} z_j \\ 0 & \sum_{j=1}^{8} \frac{\partial N_j'}{\partial q} x_j & \sum_{j=1}^{8} \frac{\partial N_j'}{\partial q} y_j & \sum_{j=1}^{8} \frac{\partial N_j'}{\partial q} z_j \end{bmatrix}$$

Substituting (20) into (18) yields the displacement shape function in terms of the global nodal variables

$$f(r,s,q) = \sum_{i=1}^{8} [N]_i[J'](f)_i = \sum_{i=1}^{8} [N^*]_i(f)_i \tag{21}$$

A complete three-dimensional state of strain is assumed for the element

$$\{\epsilon\} = \begin{Bmatrix} \epsilon_x \\ \epsilon_y \\ \epsilon_z \\ \gamma_{xy} \\ \gamma_{yz} \\ \gamma_{zx} \end{Bmatrix} = \begin{Bmatrix} \frac{\partial u}{\partial x} \\ \frac{\partial v}{\partial y} \\ \frac{\partial w}{\partial z} \\ \frac{\partial v}{\partial x} + \frac{\partial u}{\partial y} \\ \frac{\partial w}{\partial y} + \frac{\partial v}{\partial z} \\ \frac{\partial u}{\partial z} + \frac{\partial w}{\partial x} \end{Bmatrix} \qquad (22)$$

The partial derivatives in (22) are evaluated using (21), to give strains in terms of the nodal variables. Formulation of the element mass and stiffness matrices follow the same procedures used for the two-dimensional element. Similarly, average stresses and strains may be found by integrating over the volume of a ply, or the area of an interface.

By restricting the geometry of the element to be rectangular, formulation of the element matrices can be greatly simplified. Shape functions for this element may be found by substituting the identities

$$r = 2x/\ell$$

$$s = 2y/w \qquad (23)$$

$$q = 2z/t$$

into (16) and (19). The transformation from local to global nodal variables then becomes

$$\frac{\partial f_i}{\partial r} = \frac{\ell}{2} \frac{\partial f_i}{\partial x}$$

$$\frac{\partial f_i}{\partial s} = \frac{w}{2} \frac{\partial f_i}{\partial y}$$

$$\frac{\partial f_i}{\partial t} = \frac{t}{2} \frac{\partial f_i}{\partial z}$$

The computational effort required for this special case is significantly reduced relative to that required for the general element. As with the two-dimensional element, consistant mass matrices are generated for both three-dimensional elements.

3. NON-LINEAR CONTACT MODEL

The impactor is modeled as a lumped mass, coupled to the laminate through a nonlinear spring at a single node. This model is based on the work of Sun & Yang, and Yang & Sun (Ref. 4 and 5). The contact force is assumed to be a nonlinear function of the difference in the lateral displacements of the impactor and the impacted node.

When loading, the contact force is given by

$$q_I = K\Delta^n \tag{24}$$

when Δ is the difference in the lateral deflections, and K and n are empirically defined loading parameters.

When unloading, the contact force is given by

$$q_I = q_{max} \left[\frac{\Delta - \Delta_o}{\Delta_{max} - \Delta_o} \right]^m \tag{25}$$

where m is an empirical parameter, and Δ_o represents a permanent indentation in the laminate given by

$$\Delta_o = \Delta_{max}[1 - (\frac{\Delta_{cr}}{\Delta_{max}})^i] \tag{26a}$$

when Δ_{max} is greater than Δ_{cr}, and by

$$\Delta_o = 0 \tag{26b}$$

$$[K^*] = [T^*]^T[K][T^*]$$

$$\{q^*\} = [T^*]^T\{q\}$$

which are now the reduced equations of motion for the complete laminate. The effect of the reduction process is to lump all inertial effects at the governor degrees of freedom. Great care should then be exercised in selecting both master and governor degrees of freedom.

The equations of motion for the complete plate/impactor system requires the equation of motion for the impactor. Since the impactor is included as a lumped mass, its equation of motion is given by rigid body dynamics as

$$m_I\ddot{u}_I = q_I \tag{33}$$

where m_I is the mass of the impactor, u_I is its displacement, and q_I is the contact force.

The set of simultaneous differential equations given by (32) and (33) may be integrated to give the dynamic response of the complete system. This integration is most easily performed by transforming the second order differential equations into two sets of first order equations. Defining

$$\{\dot{u}_g\} = \{v_g\} \tag{34a}$$

and

$$\dot{u}_I = v_I \tag{34b}$$

Equations (33) and (32) may be solved for $\{\ddot{u}_g\}$ and $\ddot{u}_I$, yielding

$$\dot{v}_I = \ddot{u}_I = q_I/m_I \tag{35a}$$

and

$$\{\dot{v}_g\} = \{\ddot{u}_g\} = [M^*]^{-1}(\{q^*\} - [K^*]\{u_g\}) \tag{35b}$$

Combining (34a), (34b), (35a), and (35b) gives

$$\{\dot{u}'\} = \{q'\} + [D']\{u'\} \tag{36}$$

where

$$\{u'\}^T = \{u_I \quad u_g^T \quad v_I \quad v_g^T\}$$

$$[D'] = \begin{bmatrix} 0 & 0 & 1 & 0 \\ 0 & 0 & 0 & [I] \\ 0 & 0 & 0 & 0 \\ 0 & -[M^*]^{-1}[K^*] & 0 & 0 \end{bmatrix}$$

and

$$\{q'\}^T = \{0 \ \{0\}^T \ q_I/m_I \quad ([M^*]^{-1}\{q^*\})^T\}$$

Equation (36) can easily be integrated numerically using one of the Runge-Kutta algorithms, which 'step out' the dynamic response of the system, given initial displacements and velocities. The general form of these algorithms for the solution at the nth time step is

$$\{u'\}_n = \{u'\}_{n-1} + \Delta t \cdot f(t,u',\dot{u}') \tag{37}$$

where Δt is the time increment, and $f(t,u',\dot{u}')$ is an estimate of the average slope over the time interval. Explicit forms of Equation (37) are given in Reference 7.

Using (37), the displacements and velocities of the impactor and governor degrees may be stepped out to any point in time. Accelerations at this time are given by (35a) and (35b). The response of the complete set of master degrees of freedom are given by (31), allowing the response of the slave degrees of freedom to be found using (28).

FAILURE ANALYSIS

The displacement history given by (37), (31), and (28) may be used in Equations (12) and (14) to determine average ply and interface strains in each element. These strains are then used in Equation (13) and (15) to determine the corresponding stresses. Thus, the time varying spatial distributions of stress and strain are given throughout the laminate.

Damage initiation may then be determined by applying failure criteria to either the stress or strain distributions. The first criterion that is meet will determine the time and location of the onset of damage. The predicted response after the initiation on damage is then of questionable value since it will not reflect changes in stiffness which may effect the actual response. This will be discussed in further detail in the analysis section of this report.

Since all six stress components are available, it is desirable to use failure criteria that account for interactions between these components. For predicting failure within a ply, Hashin's failure criteria with slight modifications are used (Ref. 8). These criteria define distinct modes of failure for both the fiber and matrix.

The fiber tensile mode assumes a quadratic interaction between the axial stress and the maximum axial shear and is predicted when

$$\left[\frac{\sigma_1}{s_1^t}\right]^2 + \frac{(\tau_{12}^2 + \tau_{31}^2)}{S_{12}^2} = 1 \tag{38}$$

where s_1^t and s_{12} are the axial tensile and axial shear strengths respectively. This criterion is applicable when σ_1 is positive, and is used to predict a failure mode characterized by fiber breakage.

When σ_1 is compressive it is assumed that failure is characterized by fiber buckling and is only dependent upon σ_1. The compressive fiber mode failure criterion is then given by the maximum stress criterion

$$\left[\frac{\sigma_1}{s_1^-}\right]^2 = 1 \tag{39}$$

where s_1^- is the axial compressive strength of the ply.

Matrix mode failures are characterized by cracks running parallel to the fibers. Failures are described as being tensile or compressive, depending upon the sign of the quantity $(\sigma_2 + \sigma_3)$. Both matrix mode failure criteria assume quadratic interactions between the transverse stresses, both in-plane and through the thickness, the maximum shear in the transverse plane and the maximum axial shear.

When $(\sigma_2 + \sigma_3)$ is positive, the tensile mode criterion is used. This criterion is given by

$$\left[\frac{\sigma_2 + \sigma_3}{s_2^+}\right]^2 + \frac{(\tau_{23}^2 + \sigma_2\sigma_3)}{s_{23}^2} + \frac{(\tau_{12}^2 + \tau_{31}^2)}{s_{12}^2} - 1 \qquad (40)$$

where s_2^+ and s_{23} are the transverse tensile and transverse shear strengths.

For $(\sigma_2 + \sigma_3)$ negative, the compressive failure criteria is given by

$$\frac{\left[\frac{\sigma_2 - \sigma_3}{2}\right]^2 + \tau_{23}^2}{s_{23}^2} + \frac{(\tau_{12}^2 + \tau_{31}^2)}{s_{12}^2} - 1 \qquad (41)$$

which is a simple quadratic interaction between the maximum transverse and axial shears. Failure predicted by this criterion will be referred to as shear failures.

In contrast to the plies, interfaces are assumed to be homogeneous, matrix rich regions. Although orthotropic interface properties could be included in the problem formulation, commonly used matrix materials are typically isotropic, allowing the use of simpler failure criteria.

Assuming an isotropic interface, a simple criterion may be established by postulating a failure surface that is analogous to the Von Mises yield surface. Failure is then predicted by a maximum stress criterion which utilizes the octahedral shear stress (Ref. 9)

$$\frac{1}{6}[(\sigma_1 - \sigma_2)^2 + (\sigma_2 - \sigma_3)^2 + (\sigma_3 - \sigma_1)^2]/\tau - 1 \qquad (42)$$

where σ_i are principle stresses, and τ is the shear strength of the interface.

It should be noted that a number of criteria have been postulated for predicting the failure of fibrous composites. The set of criteria described above constitute only one of these. Its applicability and the applicability of any such criteria depend upon the characteristics of the materials to which they are applied, and can only be validated experimentally.

This set of criteria is then presented as one possible set which has been shown to agree well with experimental results for epoxy composites. Other criteria may be better suited for different materials and could be substituted into the framework of this analysis.

III. ANALYSIS

A number of laminated composite plates were analyzed to verify the applicability of the analytical model. These analyses included AS4/3502 plates that were tested by AFML, and IM6/934 plates that were part of another research program being performed by MSC. The AFML data were collected for a number of different support geometries and laminate configurations, whereas the IM6/934 analyses considered identical plates impacted at different velocities. The experimental data consisted of contact force histories for the impact events.

1. MODEL DESCRIPTIONS

Experimental impact data for quasi-isotropic AS4/3502 plates containing either 8 or 16 plies was made available by AFML. These plates were simply supported over 25, 50, 75 or 100 mm circles, and a pendulum impactor was used for all tests. This impact test setup is described in Reference 10. Of these plates, the 50 and 75 mm support 16 ply, and the 25, 50 and 75 mm support 8 ply were analyzed. Table 1 outlines the conditions for each of these analyses.

Ply properties for AS4/3502 were taken from References 11 and 12, and neat resin properties for 3502 were taken from 13. These properties are summarized in Table 2 and were used for all AS4/3502 analyses.

Parameters for the contact model were taken from experimental tests on a graphite/epoxy laminate conducted by Sun and Wang (14). Although the laminate used for these tests was not identical to the AS4/3502 laminate being considered here, it was assumed that the contact parameters for the two would be similar. The parameters used for the AS4/3502 analyses are summarized in Table 3.

Finite element models of both the 8 and 16 ply laminates were generated using the 3-D laminated solid element which allows arbitrary geometries in the X-Y plane. These models were constructed such that they could be constrained over a 25, 50 or 75 mm circle, as shown by the X-Y mesh for a quarter of the laminate in Figure 9. Both models utilized this mesh, and included two elements through-the-thickness.

Two quarter-plate substructures were generated, reduced and assembled into a dynamic model of half the plate. Displacement boundary conditions were then added to this model to simulate the circular support, and to enforce rotational symmetry about the center of the plate. The reduced dynamic model included 39 governor degrees of freedom.

The IM6/934 plates were quasi-isotropic 32 ply laminates, simply supported over a 76.2 mm X 127. mm rectangle as summarized in Table 4. These tests utilized a verticle drop tower, in which the height of the impactor was varied.

The finite element model generated for these analyses utilized the 3-D laminated solid element that is restricted to rectangular geometries. Development of the dynamic model for these analysis was similar to that for the AS4/3502 model where the rotational symmetry of the laminate was exploited. The quarter-plate mesh for the IM6/934 model is shown in Figure 10.

2. RESULTS

The first AS4/3205 plate analyzed was a 16 ply laminate supported over a 50 mm diameter circle. The response of this plate was stepped out over the first millisecond of the impact event using a time step of 50 nanoseconds. The displacement solution was expanded, and a stress analysis was performed every 20 microseconds.

Lateral displacement histories predicted for the impactor and impacted node are shown in Figure 11. As indicated by the slope of the impactor displacement history in this figure, the velocity of the impactor is only slightly reduced over this interval. Very little of the kinetic energy of the impactor has been transferred into the plate at this point.

The difference between the two displacement histories in Figure 11 defines the magnitude of the contact force. Althought it is not easily seen from the figure, there is a high frequency displacement component contained in the history for the impacted node. This component is more readily seen in the contact force history which is compared to the experimental contact force in Figure 12.

Good agreement is seen between the experimental and analytical contact force histories. Of particular interest is the aforementioned high

frequency component that has approximately the same frequency and peak to peak magnitude in both cases. This correlation lends credibility to the model as a whole, and justifies the use of the chosen contact parameters.

It is argued that the abrupt drop off in the experimental contact force at about 0.8 ms indicates the initiation of damage in the laminate. This point in the contact history then serves as a reference for assessing the models ability to predict the onset of damage.

The stress histories predicted by this analysis indicate tensile matrix failures developing as soon as 0.4 ms into the event. This damage is found in the bottom most ply of elements closest to the impactor. It was assumed that these failures would result in cracks in the matrix that would not significantly effect the stiffness of the laminate, and the analysis was continued. The validity of this assumption will be discussed in greater detail later in this report.

As the analysis progresses, the region experiencing tensile matrix failure increases. This continues until about 0.92 ms when a compressive matrix mode (shear) failure is predicted for the top ply in the elements nearest the impactor. From this point on, these shear failures quickly progress down toward the center of the laminate as tensile failures progress up. The validity of the solution after 0.92 ms is then very doubtful.

The development of the stress state which produces the shear failure is shown in Figure 13 which presents histories for the maximum transverse and axial shears in the top ply. From this figure it can be seen that although the failure is dominated by the maximum transverse shear, there is still a substantial contribution from the axial shear. If it is assumed that this failure produces the damage evident in the experimental contact force trace, the difference in the predicted to experimental damage initiation times is on the order of 15%. Given the uncertainty in shear strengths, this is fairly good agreement.

If this damage initiation scenario is accepted, it becomes necessary to refine the definition of damage initiation. That is, damage initiation may be taken as the first failure that is detectable upon examination of the laminate, or the first failure that is detectable through the response of the laminate. These two failures may or may not be one and the same.

Examining the IM6/934 analysis helps clarify this point. In this analysis, a quasi-isotropic plate was impacted at a velocity high enough to

develop tensile cracks, but below that necessary for the initiation of shear failures. The analytical contact force history predicted by this analysis is shown in Figure 14, along with the point at which damage initiation was predicted.

As with the AS4/3502 plate, this initial damage is a tensile matrix mode failure in the bottom most ply. Proprietary experimental results for this plate showed no evidence of damage in the contact force history. Post examination of the plate did, however, show visable cracks on the back surface. Damage was then initiated in the plate, but did not effect its dynamic response.

This plate was also analyzed at higher impact velocities, for which the damage initiation scenario was similar to that of the IM6/3502 plate. These analyses correlated very well with proprietary experimental results for both the contact force history and the damage initiation times.

These analyses both verified the existence of tensile cracks early in the dynamic response, and validated the use of the analytical model after these cracks were predicted. Analysis of the AS4/3502 plates was then resumed.

The next case considered was a 16 ply plate supported over a 75 mm circle. The response of this plate was similar to the 50 mm support case, and followed the same damage scenario. The experimental and analytical contact force histories for this case are compared in Figure 15. As shown in the figure, damage consists of the formation of tensile cracks followed by shear failures in the top ply. Throughout the remainder of this report damage initiation will be interpreted as the initiation of failures which influence the dynamic response.

Eight ply AS4/3502 plates, supported over 25, 50 and 75 mm circles, were the final analyses performed. Experimental and analytical contact force histories for these cases are shown in Figures 16, 17 and 18 respectively. In all cases, the formulation of damage was similar to that seen in the 16 ply plates.

Analytical results for the 25 mm support case correlate well with the magnitude of the experimental contact force up to the time of damage initiation. The 50 and 75 mm support cases, however, only correlate through the first millisecond of the response and then diverge. This implies that

there is considerable membrane stretching in these plates, a non-linear effect that is not included in the formulation of the model.

This is verified by examining the magnitudes of the extensional strains predicted by the linear formulation. Using the displacement solution for the node on the back surface of the plate at X = 2.54 mm, Y = 0.0 mm, global strains were calculated using both the linear and non-linear definitions of strain. Since first derivatives of the displacements are included as nodal degrees of freedom, the linear strains are found directly, and the non-linear strains are easily calculated.

The dominant extensional strain at this point is the strain in the Y direction. Histories for the linear and non-linear formulations of this component are shown in Figure 19. As expected, the two curves do diverge. It should be noted, however, that the non-linear curve is calculated from a displacement solution predicted by the linear theory. A different curve will result if the non-linear theory is used throughout the analysis, but a similar conclusion is expected.

IV. DISCUSSION AND CONCLUSIONS

The analyses included in the program have helped to define the limits of applicability of the analytical model, and have shown it to be an accurate engineering tool when used within these limits. The model is particularly well suited for the analysis of plates with low aspect ratios which typically exhibit significant shear deformation. This deformation can be characterized very well by the higher order (cubic) displacement shape functions used in the laminated solid elements.

Thinner plates will exhibit stiffening due to membrane stretching, much like the stiffening of a drum head as it is tightened. This non-linear effect can only be included by utilizing a higher order definition of strain as opposed to a higher order shape function. Although the use of the non-linear strain tensor in a finite element is well defined, in practice, it presents severe problems since it necessitates reformulating the stiffness matrix periodically. If, however, thin plates are to be analyzed, the non-linear formulation must be considered.

By qualitatively comparing the aspect ratio of each plate analyzed to the degree of correlation between the experimental and analytical contact force histories, an upper limit on the aspect ratio can be determined. Table 5 lists the aspect ratios for each of the plates considered in this program. For circular plates, the aspect ratio is taken as the ratio of the diameter to the thickness; for the rectangular plate, major and minor aspect ratios are given by the ratios of the major and minor support lengths to the thickness respectively.

Good agreement was found between the experimental and analytical contact force histories for the 50 and 75 mm support, 16 ply AS4/3502 plates; the 25 mm support, 8 ply AS4/3502 plate; and the IM6/934 plate. All of these plates had aspect ratios less than 40. The remaining plates had aspect ratios greater than 40, and did not show as good an agreement with the experimental data. An aspect ratio of about 40 is then assumed to be the upper limit for which the model is appropriate.

All analyses predicted matrix cracking in plies on the tensile side of the laminate early in the response. The existence of these cracks has been verified in unpublished proprietary data and has no effect on the dynamic response of a plate. The analytical response was then considered valid up to

the point at which a failure occurred that would effect the dynamic response. For all cases considered, this failure was due to the shear stress in the top ply on the compressive side of the laminate. In this regard, the model can track damage to a limited extent.

It must be noted that the findings of these analyses are for a specific impactor and may not hold for different impactors even when the impact energy is the same. The response of the plate/impactor system depends upon the dynamics of both parts. Changing the mass of the impactor changes its dynamics and, therefore, changes the dynamics of the system.

To demonstrate this, it is beneficial to consider the response of a system in generalized coordinates. With this formulation, the response is given by

$$u(x,y,z,t) = \sum_{i=1}^{n} C_i(t) \cdot \phi_i(x,y,z) \qquad (43)$$

where the ϕ are eigenvectors of the system, and the C's are generalized coordinates. The first eigenvector characterizes a rigid body motion of the impactor, the second is the first mode of the plate, the third is the second mode of the plate, and so on.

Time histories for the second through ninth generalized coordinates of an IM6/934 analysis are shown in Figure 20. The impact scenario for this analysis is a large mass traveling at a low velocity. From this figure, it can be seen that the response of the plate is primarily a first mode response with a small second mode contribution. In contrast to this, Figure 21 shows the generalized coordinates for the same plate being impacted by a small mass at a higher velocity. The impact events for these analyses are summarized in Table 6. Note that the impact energy is the same for both.

There are many differences in the predicted responses for these two cases, the most obvious being the participation of higher modes than the second. The initiation of damage in the second case is also quite different. As in the analysis for the large impactor, the first failure predicted in the small mass analysis is matrix cracking in the tensile side, followed by shear failure in the compressive side. In the first analysis, the matrix cracking is predicted at about 500 microseconds while it occurs around 25 microseconds for the second. Similarly, the first analysis

predicted the shear failure at about 1350 microseconds compared to 35 microseconds for the second.

More important than the times at which these failures are predicted, are the locations at which they occur. The large mass analysis predicts the shear failure in the upper most ply of the laminate, whereas the small mass analysis predicts it for the third ply in from the top surface. Both analyses predict tensile cracking in the bottom most ply. The difference in the predicted damage location means that the spatial stress distribution is dependent upon the mass of the impactor, as is the temporal distribution.

The contribution of higher modes in the small mass analysis is important to the displacement response of the plate, but is of even more importance in defining the stress and strain response. The higher frequencies are associated with modes characterized by shorter wave lengths resulting in higher curvatures. The magnitude of the generalized coordinate multiplying such a mode may then be relatively small and still have a substantial contribution to the stress distribution.

For example, consider the bending response of a simply supported uniform beam. Neglecting shear deformation and rotary inertia, the eigenvalues for this beam are given by

$$\omega_i = (i\,\pi^2) \cdot EI/mL^4 \tag{44}$$

where E is the axial modulus, I is the bending moment of inertia, m is the mass of the beam, and L is its length. The eigenvectors associated with these eigenvalues are

$$w_i(x) = 2/mL \cdot \sin(i\,\pi\,x/L) \tag{45}$$

From (43), the general response of the beam is then

$$w(x,t) + \sum_{i=1}^{\infty} C_i(t) \cdot w_i(x) \tag{46}$$

The bending stress in this beam is given by

$$\sigma_x = -Ez \frac{\partial^2 w}{\partial x^2} \tag{47}$$

Substituting 45 and 46 into 47 gives

$$\sigma_x = E\, z \sum_{i=1}^{\infty} C_i(t) \left[2/mL \cdot (i\,\pi/L)^2 \cdot \sin(i\,\pi\, x/L) \right] \tag{48}$$

Considering the contribution of the first two symmetric modes (i=1 and i=3) to the total stress shows the importance of the generalized coordinate. The contribution from the first mode is given by

$$\sigma_{x_1} = E\, z\, C_1(t)\ \ 2/mL\ (\pi/L)^2 \sin(\pi\, x/L) \tag{49}$$

and for the third mode by

$$\sigma_{x_3} = 9\, E\, z\, C_3(t)\ \ 2/mL\ (\pi/L)^2 \sin(\pi\, x/L) \tag{50}$$

Comparing (49) to (50) it can be seen that the generalized coordinate for the third mode can be nine times smaller than that for the first mode, and still have a contribution to the stress distribution that is of the same order of magnitude as the contribution from the first. The comparison with yet higher modes becomes even more striking as the contribution from a given mode is a function of i squared. A similar expression could be developed for the bending modes of a plate.

The generalized coordinate comparison points out a fundamental problem in understanding low velocity impact. A large number of variables are associated with the problem, each of which may or may not strongly influence the response of a given laminate. It is doubtful that any one independent variable, such as initial impact energy, can be defined that will be a robust measure for the comparison of laminates. Care must then be taken to design impact tests that are representative of the expected impact scenario in service.

It may be possible that, for a given laminate, an impact test may be devised for which that specific laminate performs very well. A more informative approach to the problem is to define the range of impact scenarios for which a given laminate performs well, knowing that the definition of 'performs well' is also somewhat vague.

The analytical model developed in this program can be very beneficial if this approach is used. The impactor parameters, most notably mass and initial velocity, can be easily varied, allowing the analysis of a wide range of impact events. These analyses can then be used to identify the type of application for which this laminate is suited. As with any analytical program, a number of select cases should also be tested experimentally as a check on the numerical results.

A number of extensions to the existing model are possible and should be considered for further development. Most important is the use of a non-linear formulation for the analysis of thin plates followed by including mechanisms for tracking damage. As previously mentioned, this first extension is well defined and poses no insurmountable analytical problem. It does, however, require the use of the fastest computer available.

The second extension is not so clear cut, and does pose some significant analytical challenges. Modifying ply properties to account for matrix cracking or even fibers breaking is fairly routine, but predicting the growth of a crack is not. Finite element methods for predicting the growth of a crack have been developed (Reference 15 and 16), but are quite complex even for static loads. The nature of the cracks that develop due to low velocity impact further complicate the issue since they are trans-ply rather than inter-ply cracks.

The accumulation of damage in some laminates may occur in almost discrete steps with a damage zone being initiated and fully developed over a very short period of time. An approximate model which exploits this effect may be postulated for tracking damage in these laminates. In this model the initial stiffness of the laminate would be used to predict the response up to the initiation of a shear crack. A fracture mechanics model would then be used to predict the growth of the crack up to the point at which it became stable. A new laminate stiffness would be formulated which included the damage zone, and used to predict the dynamic response up to the next

damage initiation. Obviously, this is a simplified approach to a very complex problem but may warrant a feasibility study.

It is recommended that any further extensions of the existing model be made on the two-dimensional case. It is not obvious that results predicted by the three-dimensional model will yield any information about a laminate that is of a more general nature than 2-D results. Of course there are problems associated with the testing of beams, such as edge effects, but the reduced analytical effort is very attractive. At the very least, the 2-D model could be extended for performing feasibility studies before expending the resources on the complete 3-D formulation.

REFERENCES

1. Goering, J., "Initial Impact Damage of Composites - Phase I," MSC TFR 1601/1205, April 1985.

2. Goering, J., "Initial Impact Damage of Composites - Phase II," MSC TPR 1708/1207, May 1986.

3. Webster, W. D., Jr. "An Isoparametric Finite Element With Nodal Derivatives," ASME Paper No. 81-APM-1.

4. Sun, C. T., and Yang, S. H., "Contact Law and Impact Response of Laminated Composites," NASA CR-159884, 1980.

5. Yang, S. H., and Sun, C. T., "Indentation Law for Composite Laminates," NASA CR-165460, 1981.

6. Zienkiewicz, O. C., "The Finite Element Method," Third Edition, McGraw-Hill, 1977.

7. Carnahan, B., Luther, H. A., and Wilkes, J. O., "Applied Numerical Methods," John Wiley & Sons, 1969.

8. Hashin, A., "Failure Criteria for Unidirectional Fiber Composites," Journal of Applied Mechanics, Vol. 47, June, 1980.

9. Fung, Y. C., "Foundations of Solid Mechanics," Prentice-Hall, 1965.

10. Cordell, T. M., and Sjoblom, P. O., "Low Velocity Impact Testing of Composites," Proceedings of the American Society for Composites, First Technical Conference, 1986.

11. Zimmerman, R. S., and Adams, D. F., "Mechanical Properties of Neat Polymer Matrix Materials and Their Unidirectional Carbon fiber-Reinforced Composites," University of Wyoming, Dept. Report, UWME-DR-601-103-1.

12. Anon. "Magnamite AS4/3502 Graphite Prepreg Tape and Fabric Module," Vendor data, July 1985.

13. Zimmerman, R. S., Adams, D. F., and Walrath, D. E., "Investigation of the Relations Between Neat Resin and Advanced Composite Mechanical Properties, Volume I - Results," NASA CR-172303, May 1983.

14. Sun, C. T., and Wang, T., "Dynamic Responses of a Graphite/Epoxy Laminated Beam to Impact of Elastic Spheres," NASA CR- 165461, September, 1982.

15. Chatterjee, S. N., Ramnath, V., Pipes, R. B., and Dick, W. A., "Composite Defect Significance," MSC TFR 1507/1109.

16. Grady, J. E., and Sun, C. T., "Dynamic Delamination Crack Propagation in a Graphite Epoxy Laminate," ASTM STP 907, 1986.

Table 1. AS4/3502 Analysis Summary

Analysis	Plies*	Support Diameter (mm)	Impactor Mass (kg)	Impactor Velocity (m/s)
1	16	50	2.49	1.56
2	16	75	5.04	1.56
3	8	25	2.49	1.56
4	8	50	2.49	1.56
5	8	75	2.49	1.56

* 8 ply laminate - [0,+45,-45,90]s
16 ply laminate - [0,+45,-45,90]2s

Table 2. Material Properties for AS4/3502 Analyses

Unidirectional Ply Properties:

E_1 - 130.3 GPa

E_2 - 9.65 GPa

ν_{12} - 0.35

ν_{23} - 0.40

G_{12} - 5.93 GPa

ρ - 4.08×10^{-3} g/cc

t - 0.13 mm

S_1^T - 1793. MPa

S_1^C - 1724. MPa

S_2^T - 64. MPa

S_2^C - 138. MPa

S_{12} - 109. MPa

S_{23} - 69. MPa

Neat Resin Properties:

E - 3.79 GPa

ν - 0.36

ρ - 3.27×10^{-3} g/cc

S_1^T - 38. MPa

S_1^C - 69. MPa

S_1^2 - 62. MPa

Table 3. Contact Law Parameters for AS4/3502 Analyses

$K = 1.07 \times 10^5 N/mm^{3/2}$

$n = 1.5$

$m = 2.5$

$\Delta cr = 0.08$ mm

$i = 0.4$

Table 4. IM6/934 Analysis Summary

Analysis	Plies*	Support (mm)	Impactor Mass (kg)	Impactor Velocity (m/s)
1	32	76.2 X 127.0	3.17	1.10

* [0,90,+45,-45]4s

Table 5. Aspect Ratio Summary

Laminate	Thickness (mm)	Support (mm)	Aspect Ratio
AS4/3502	2.1133 (16 ply)	50 (Dia.)	25
AS4/3502	2.1133 (16 ply)	75 (Dia.)	35
AS4/3502	1.0566 (8 ply)	25 (Dia.)	24
AS4/3502	1.0566 (8 ply)	50 (Dia.)	47
AS4/3502	1.0566 (8 ply)	75 (Dia.)	71
IM6/934	4.1453 (32 ply)	76.2 X 127.0	18 X 31

Table 6. Generalized Coordinate Analysis Summary (IM6/934)

Analysis	Support (mm)	Impactor Mass (kg)	Impactor Velocity (m/s)	Impact Energy (N-m)
1	76.2 X 127.0	3.17	1.56	3.84
2	76.2 X 127.0	0.016	21.77	3.84

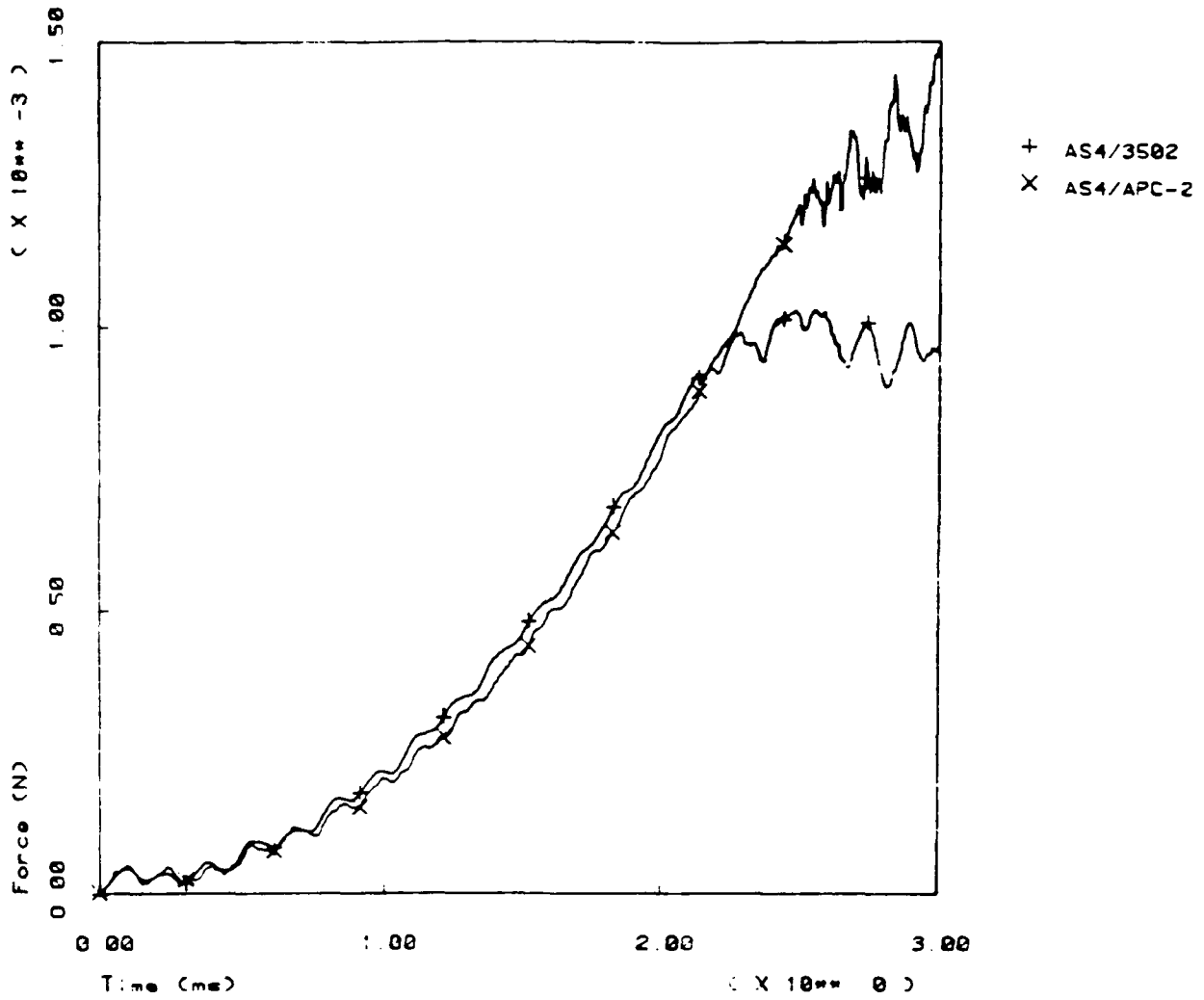

Figure 1. Experimental Contact Force History Comparison for 8 Ply Laminates With 75 mm Diameter Support

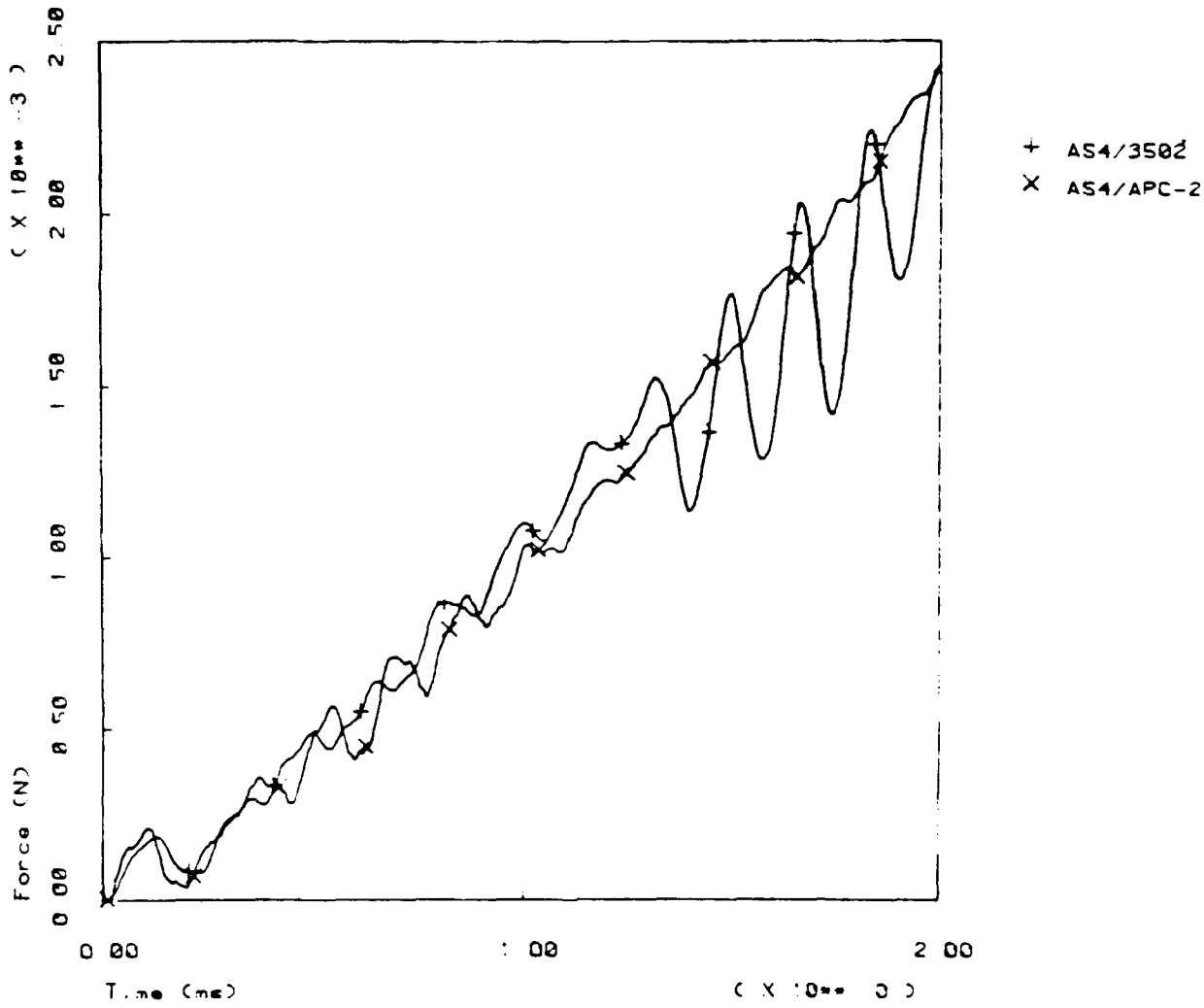

Figure 2. Experimental Contact Force History Comparison for 16 Ply Laminates With 75 mm Diameter Support

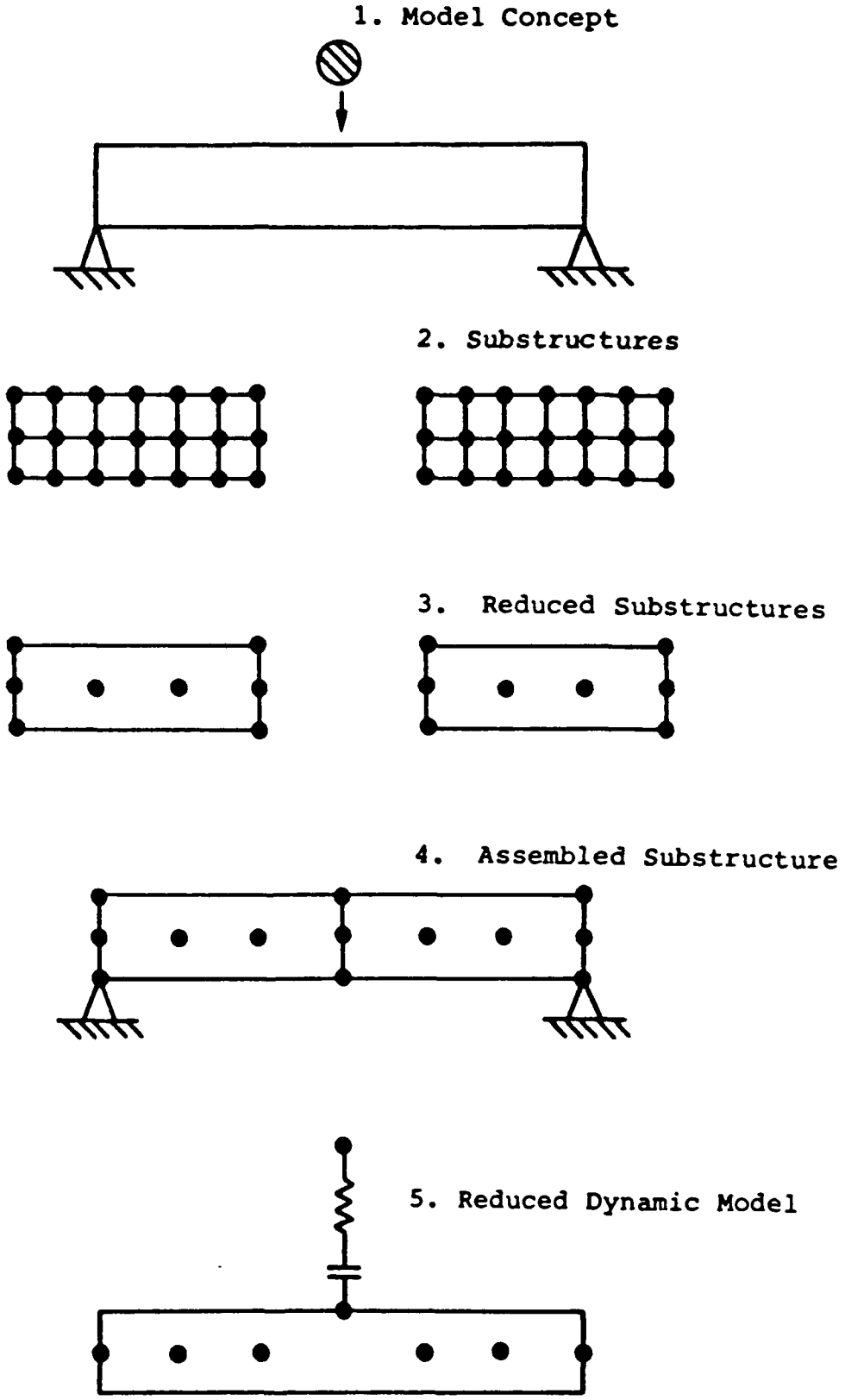

Figure 3. Model Building Sequence

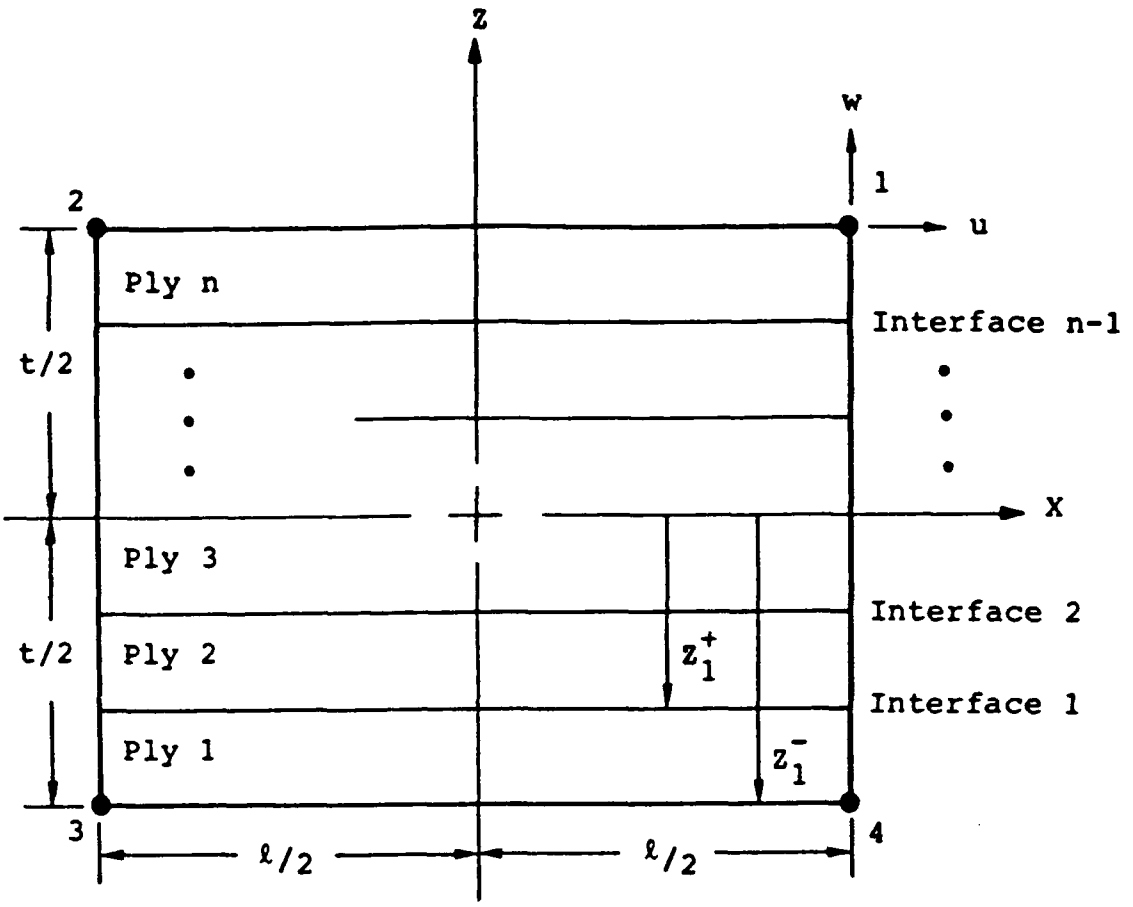

Figure 4. 2-D Element Nomenclature

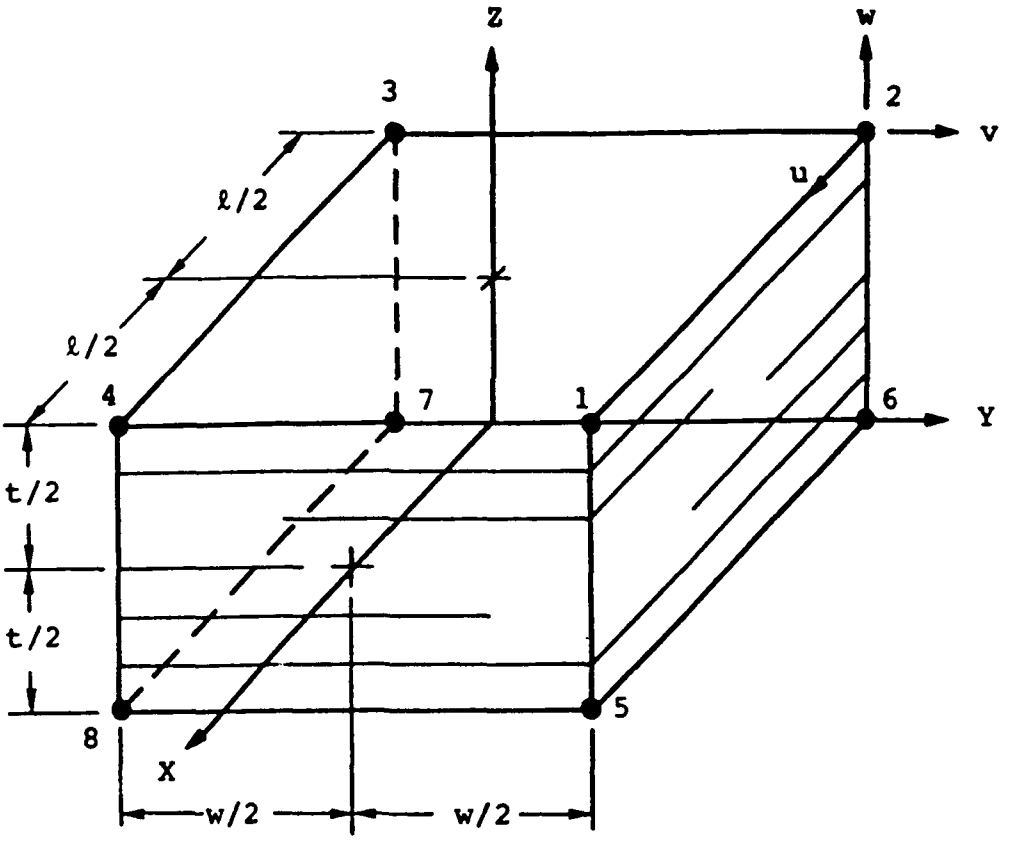

Figure 5. Special 3-D Geometry

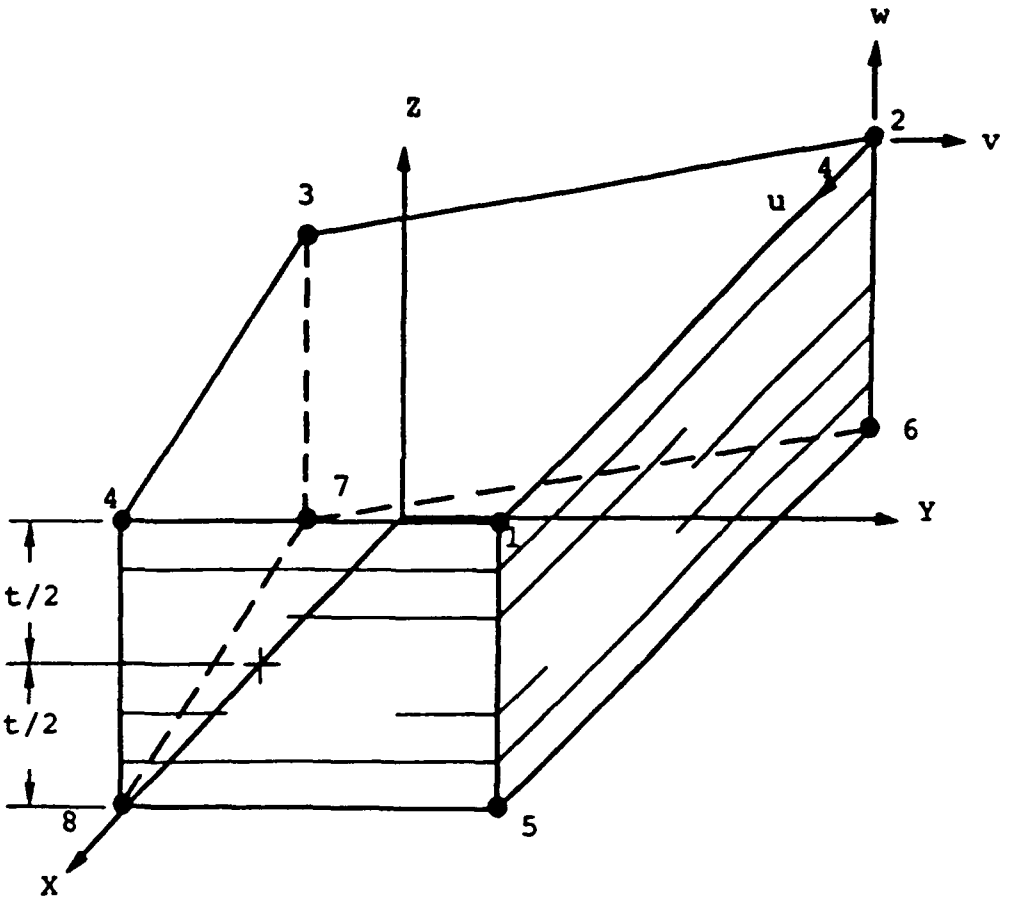

Figure 6. General 3-D Geometry

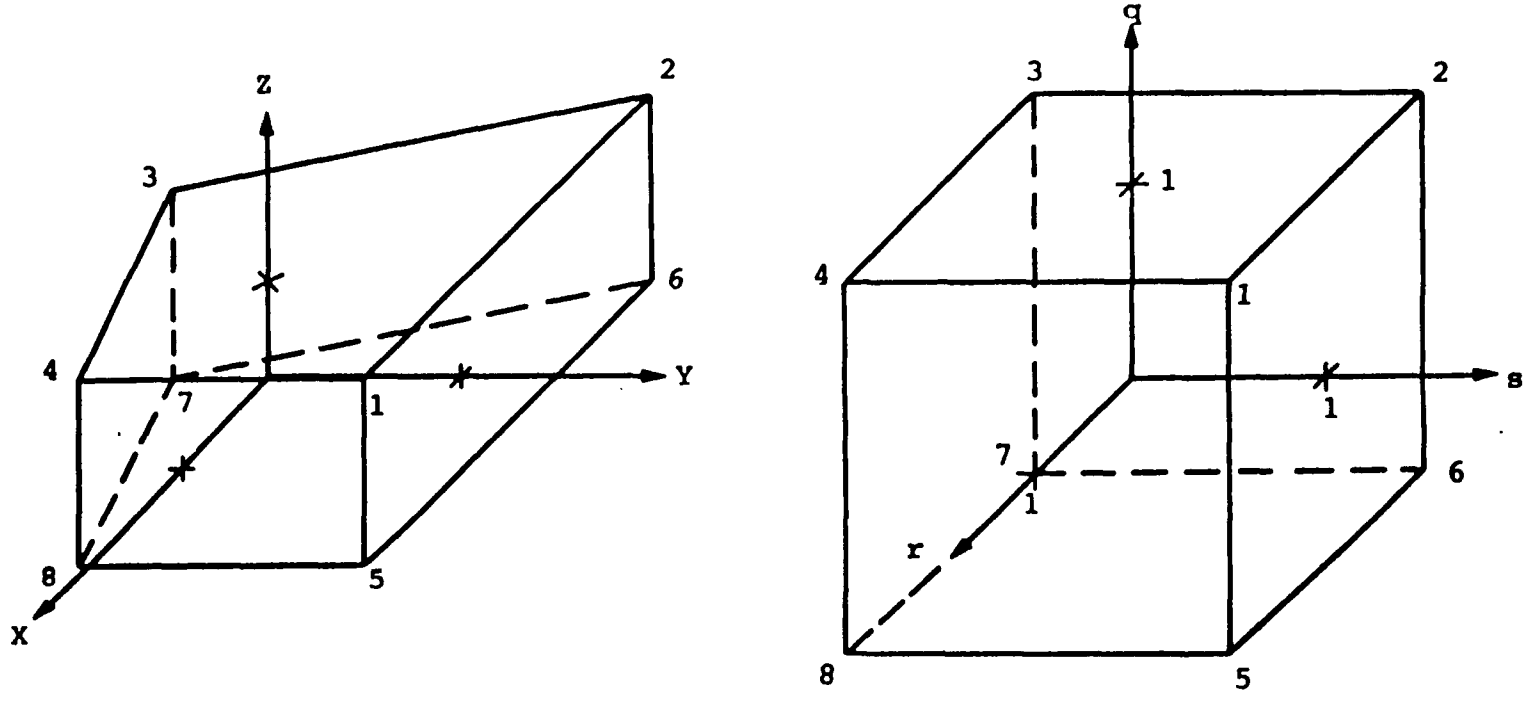

Figure 7. Local Coordinate Mapping

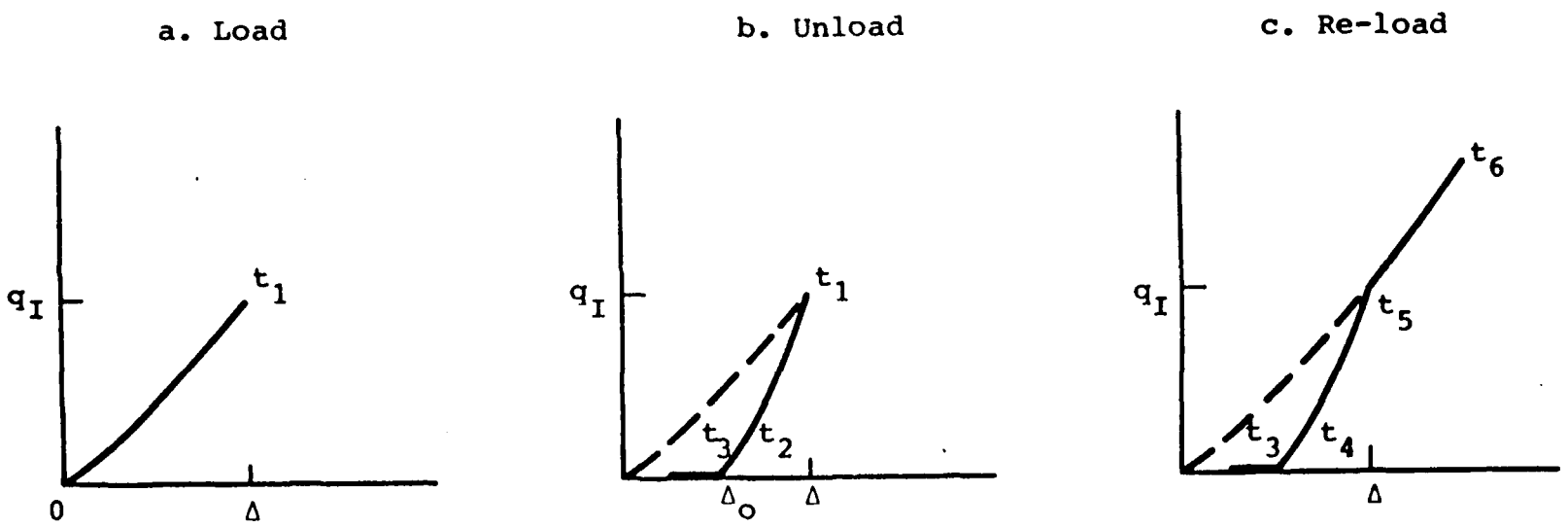

Figure 8. Typical Force-Deflection Diagram for the Contact Spring

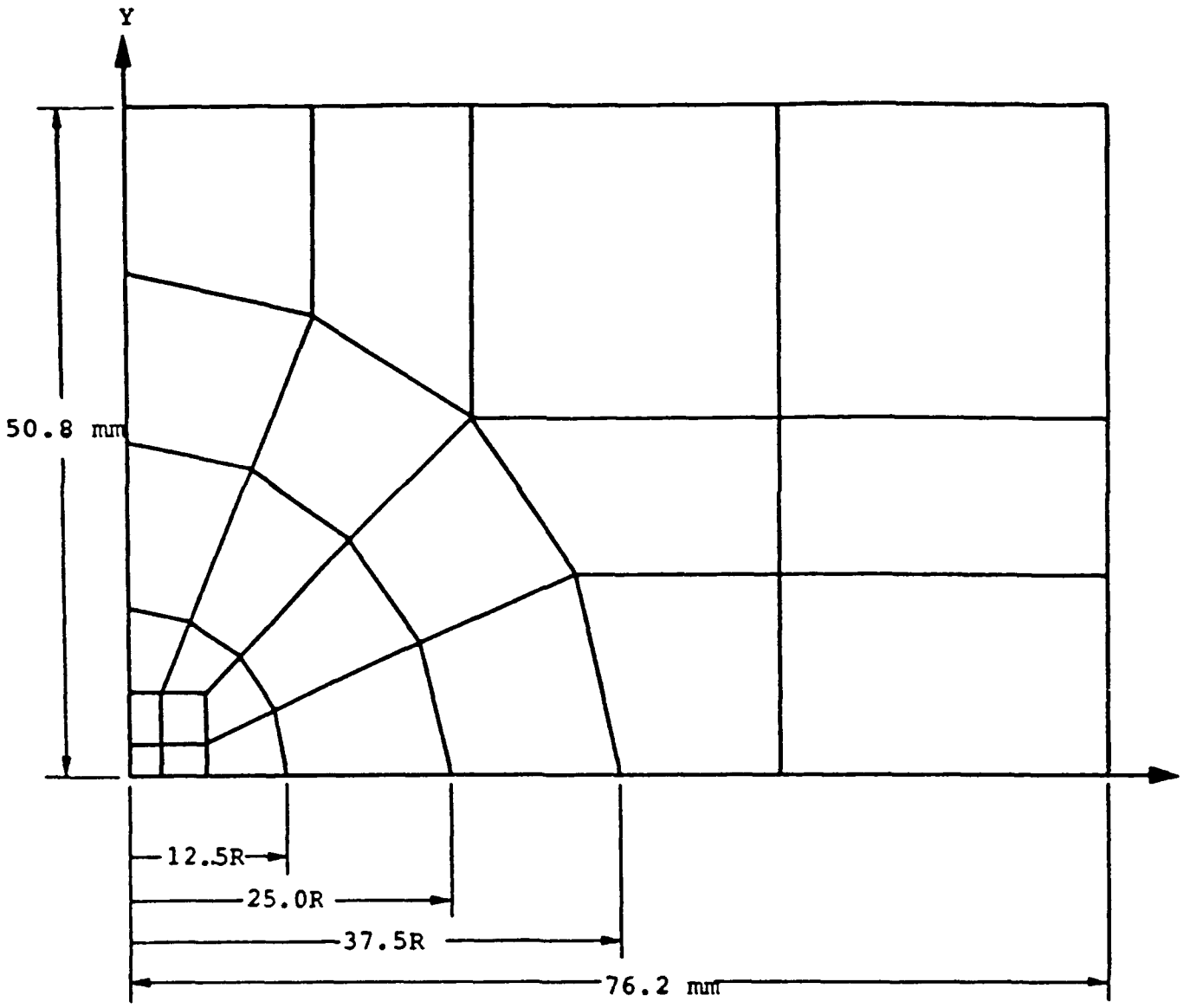

Figure 9. AS4/3502 1/4 Plate Model

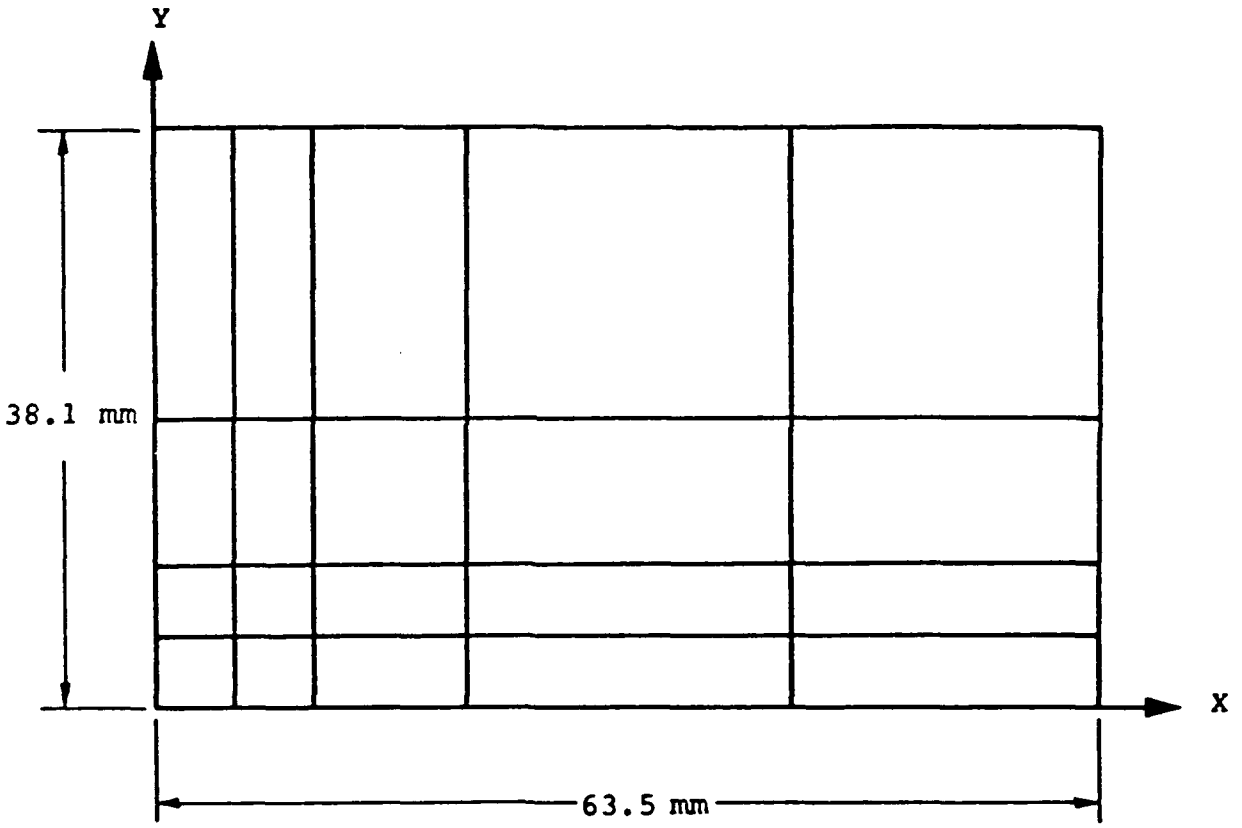

Figure 10. IM6/934 1/4 Plate Model

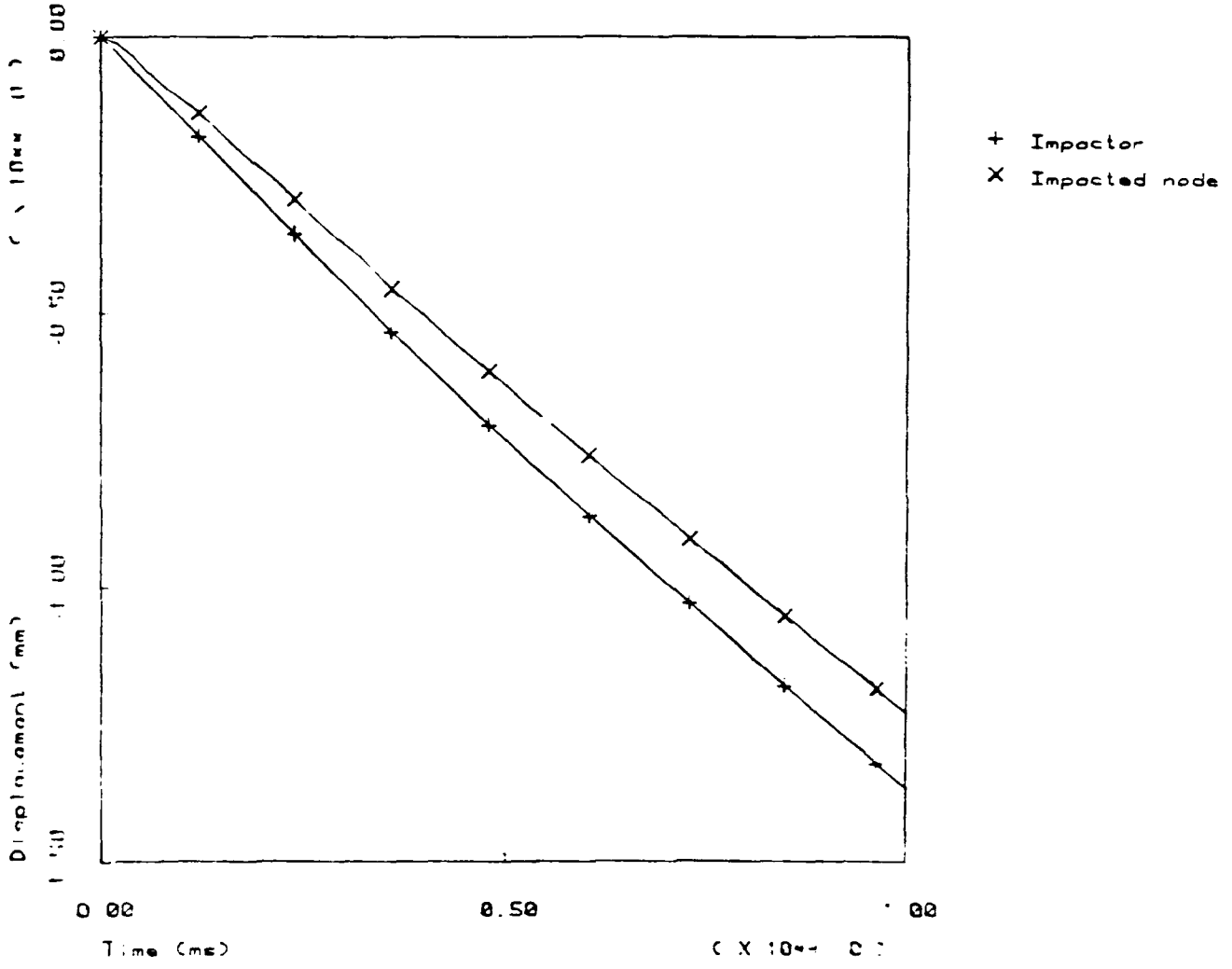

Figure 11. Impactor and Impacted Node Displacement Histories for 16 Ply AS4/3502 Laminate with 50 mm Diameter Support

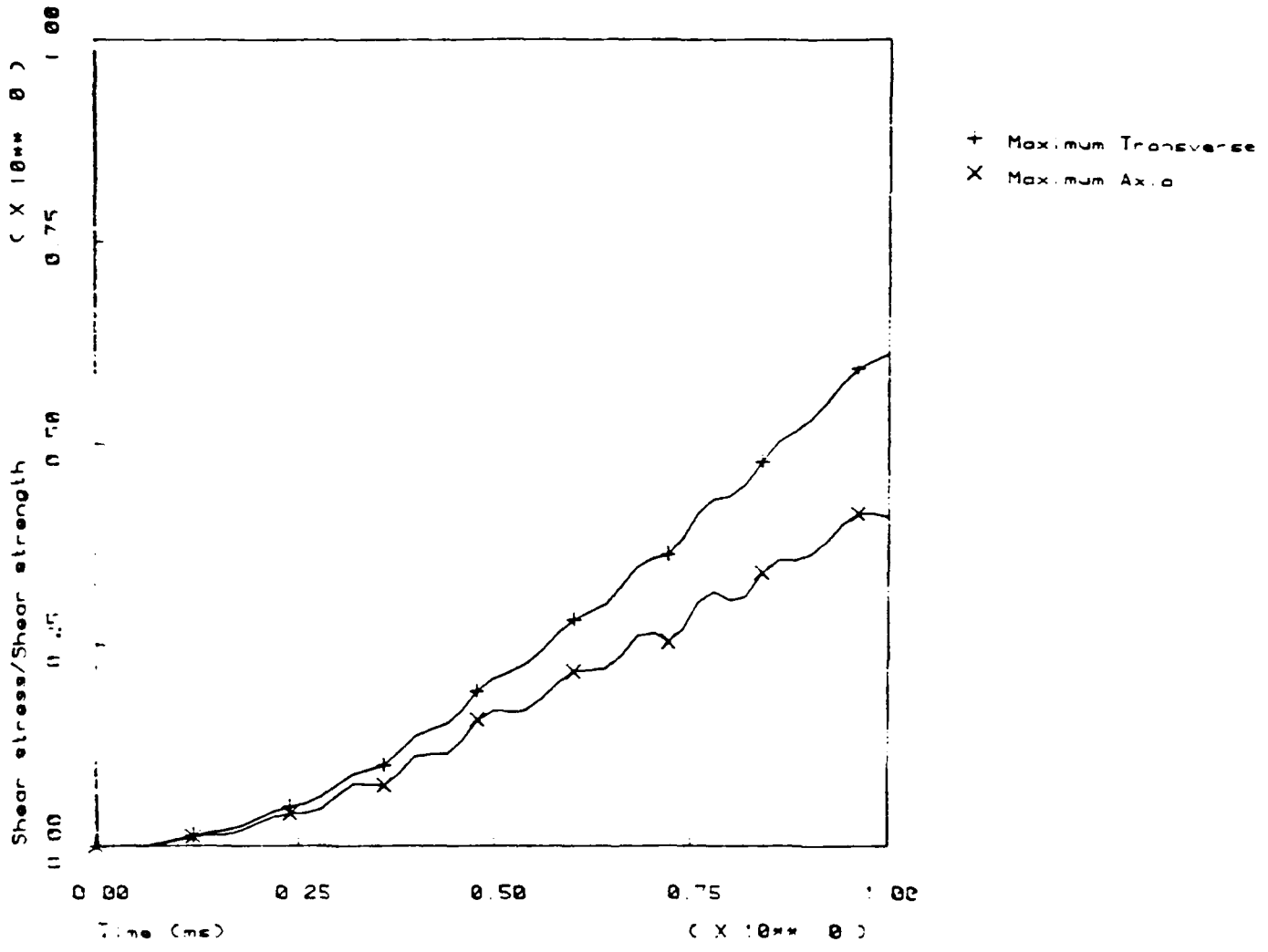

Figure 13. Normalized Stress Histories for 16 Ply AS4/3502 Laminate with 50 mm Diameter Support

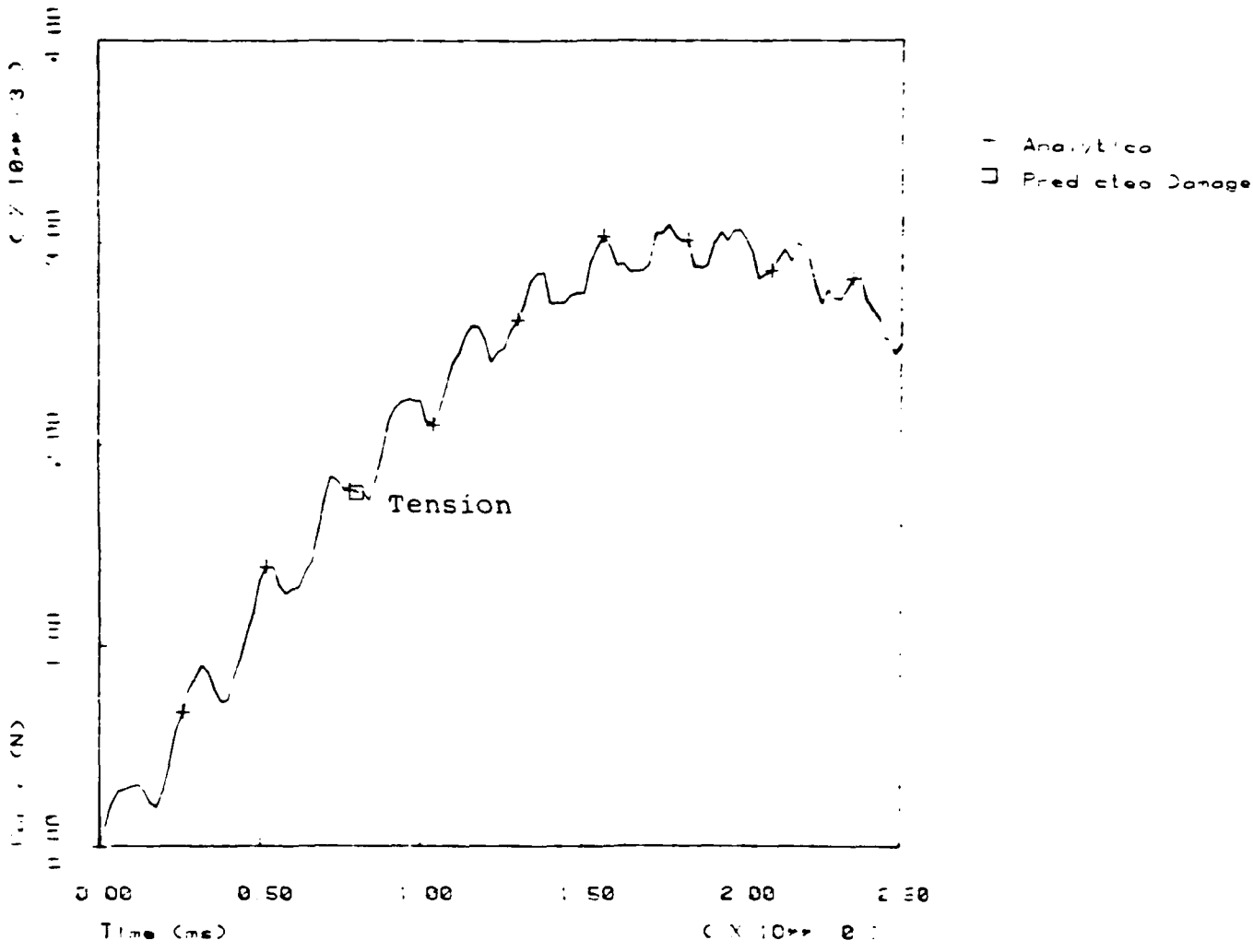

Figure 14. Contact Force History for IM6/934 Laminate. Impact Energy = 1.92 N-m.

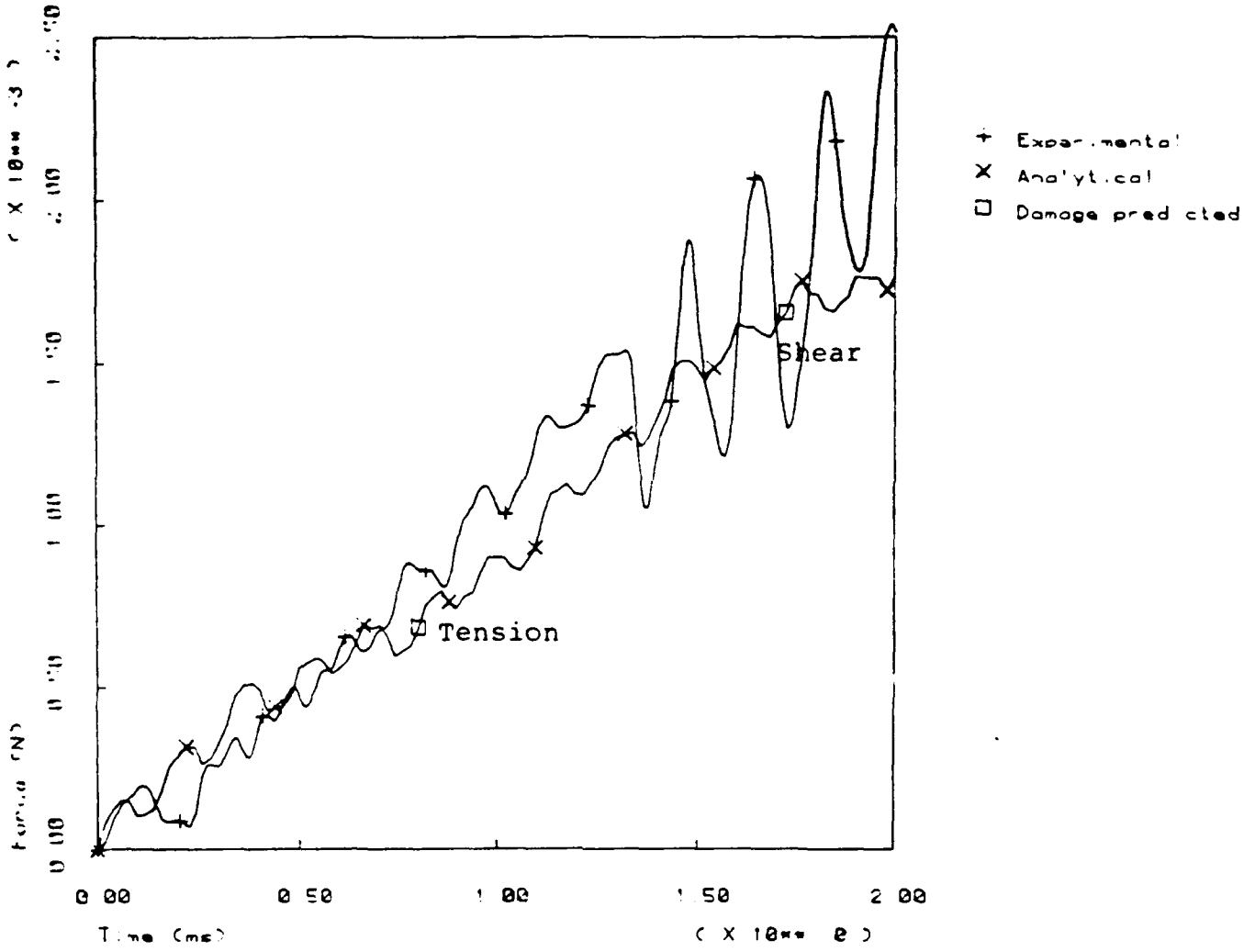

Figure 15. Contact Force History for 16 Ply AS4/3502 Laminate with 75 mm Diameter Support

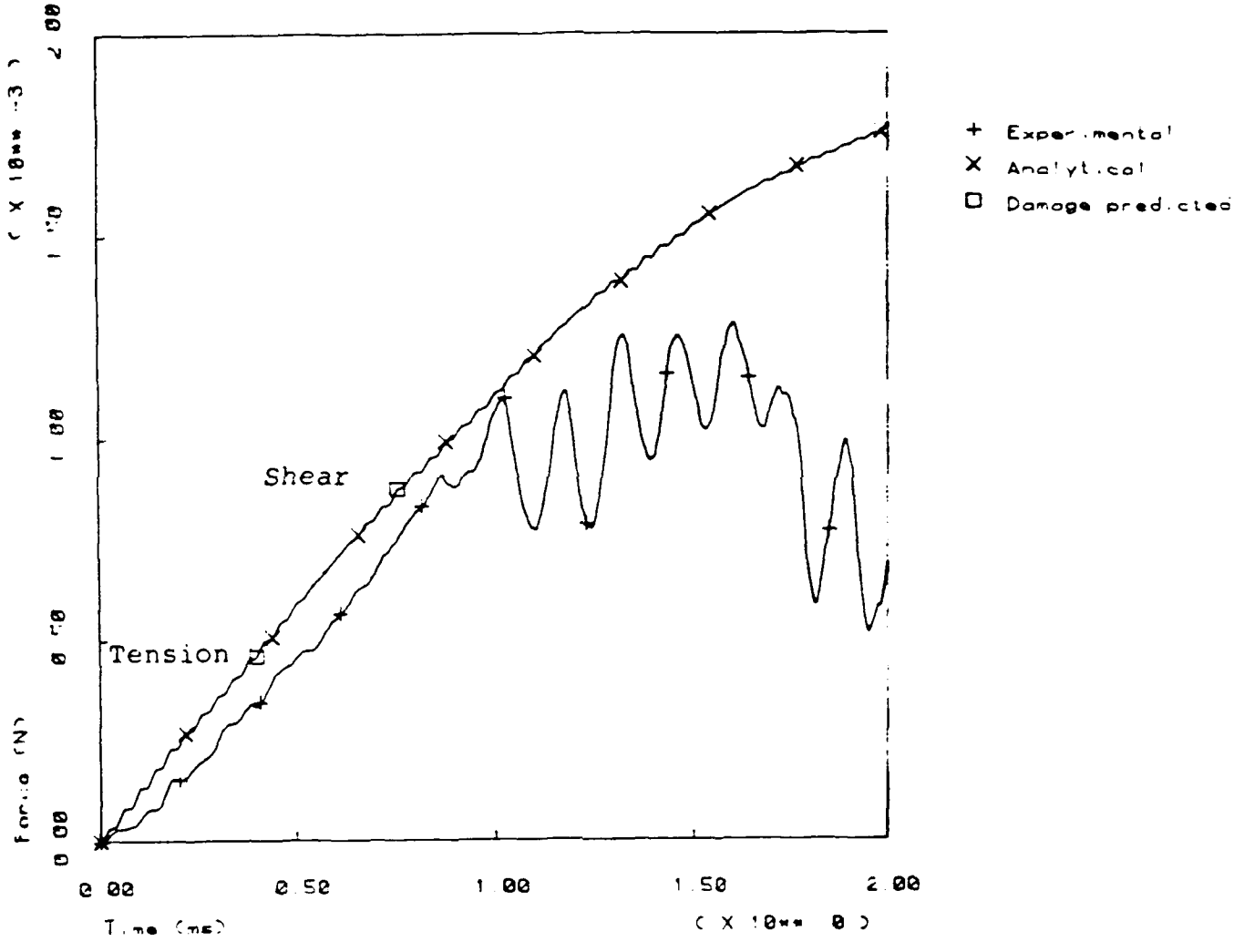

Figure 16. Contact Force History for 8 Ply AS4/3502 Laminate with 25 mm Diameter Support

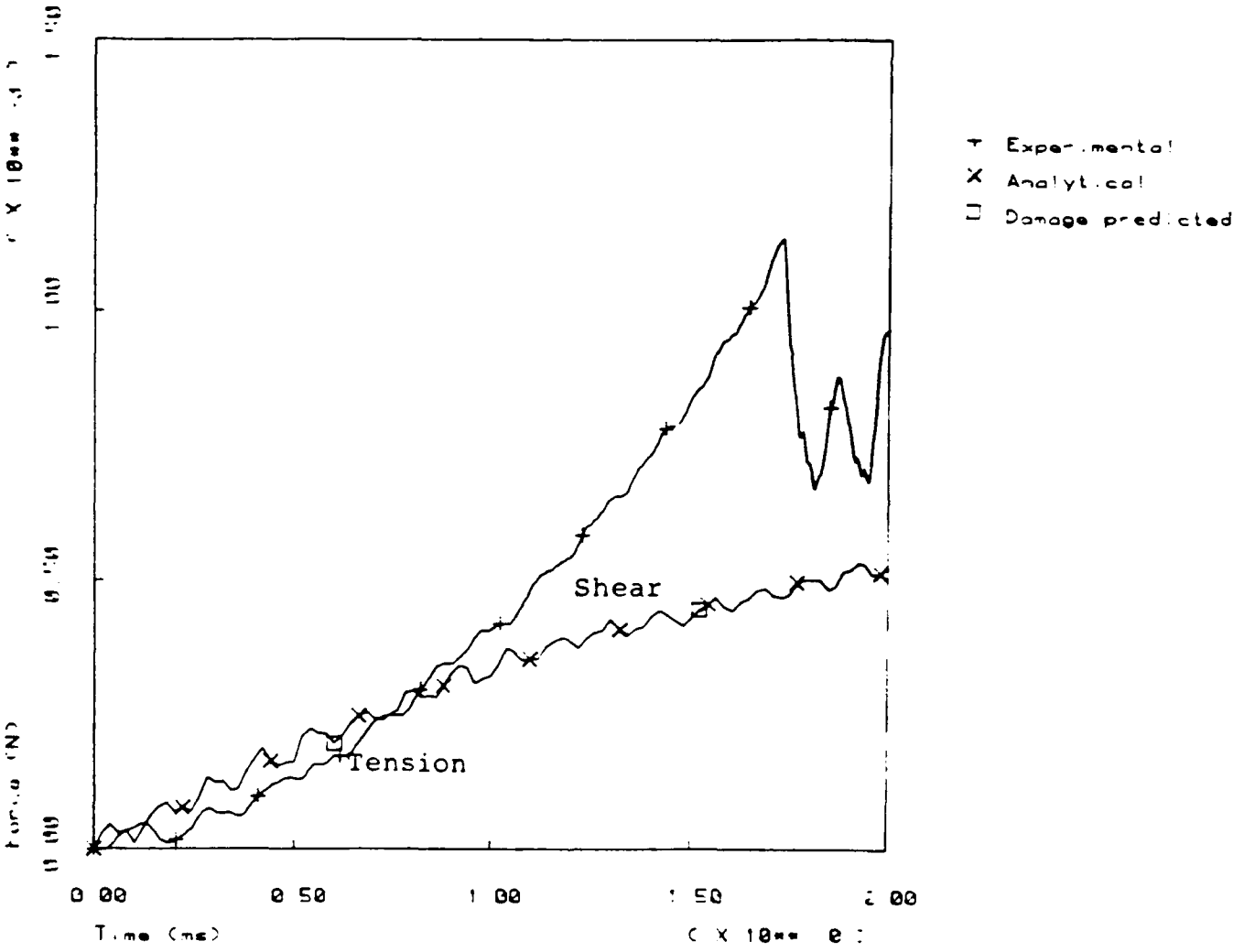

Figure 17. Contact Force History for 8 Ply AS4/3502 Laminate with 50 mm Diameter Support

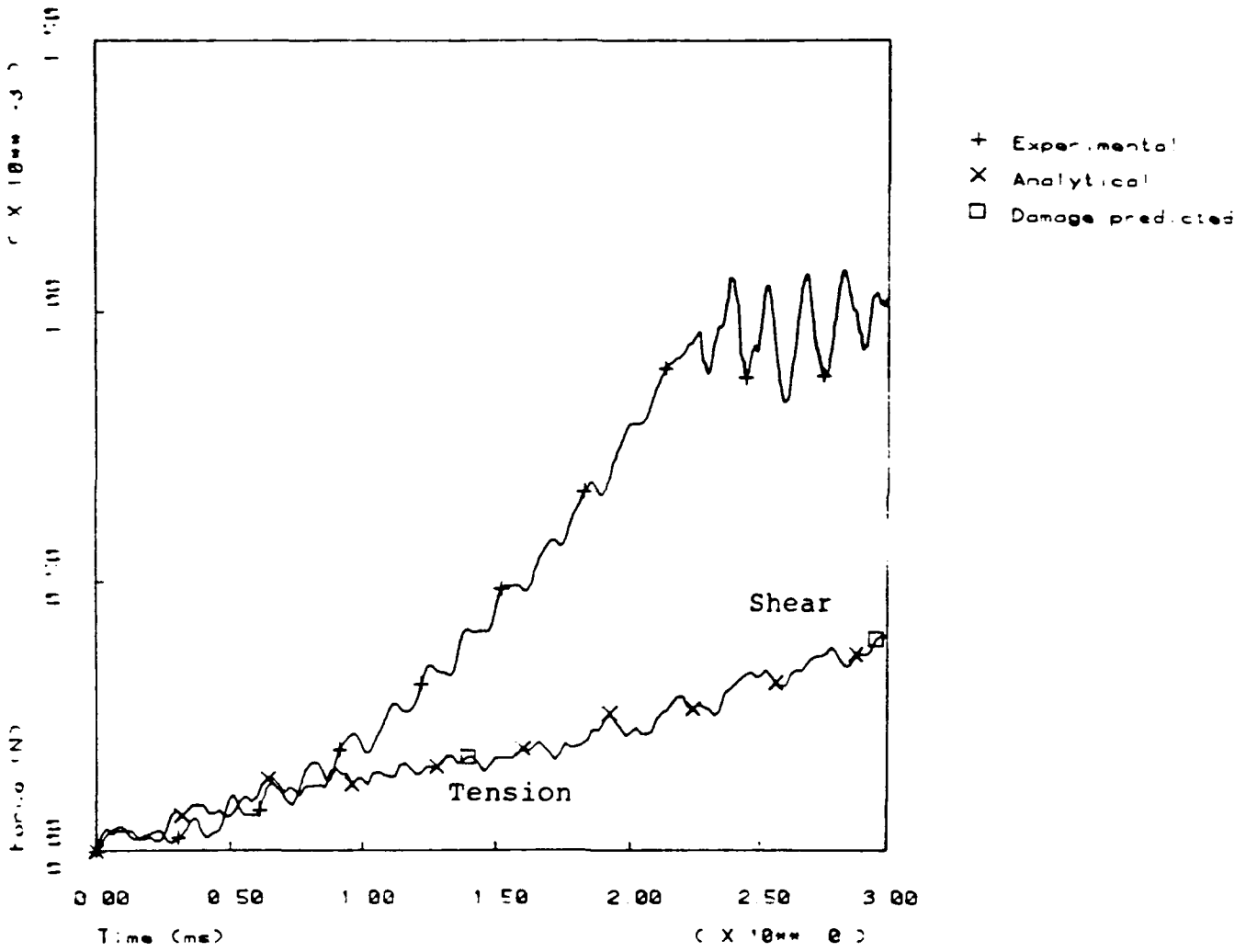

Figure 18. Contact Force History for 8 Ply AS4/3502 Laminate with 75 mm Diameter Support

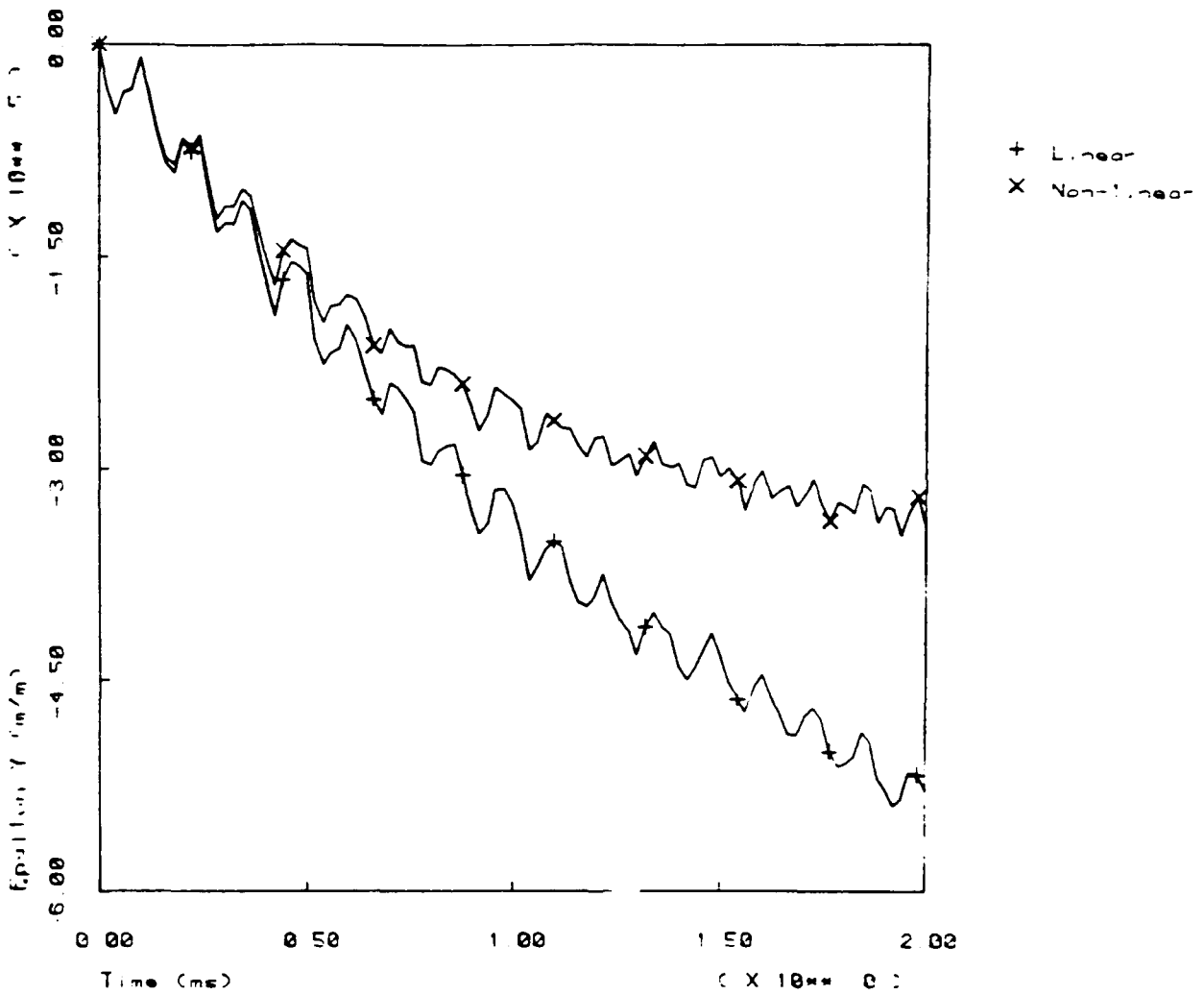

Figure 19. Extensional Strain Comparison for 8 Ply AS4/3502 Laminate with 50 mm Diameter Support

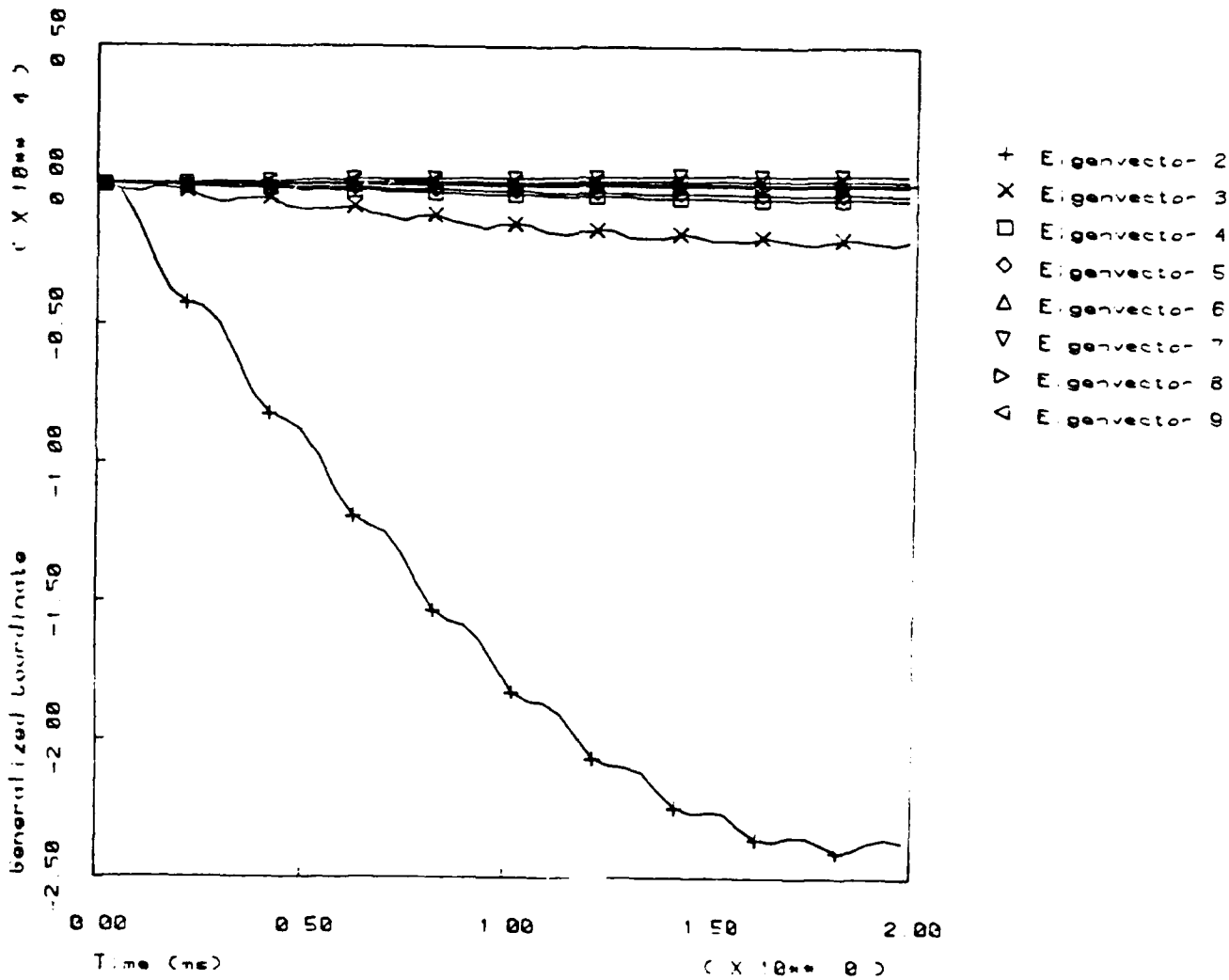

Figure 20. Generalized Coordinates for IM6/934 Laminate with Large Mass Impactor. Impact Energy = 3.84 N-m.

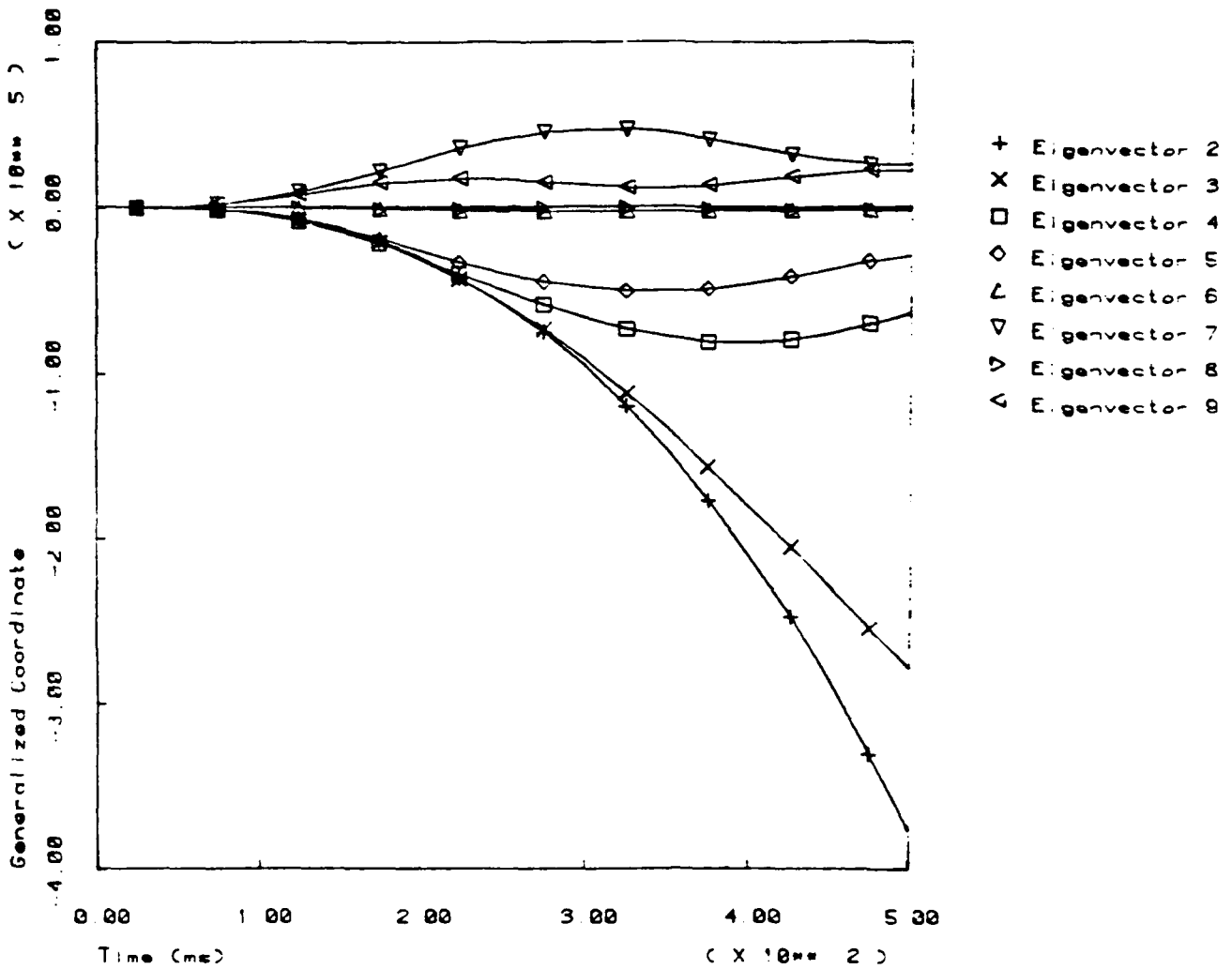

Figure 21. Generalized Coordinates for IM6/934 Laminate with Small Mass Impactor, Impact Energy = 3.84 N-m.

APPENDIX - SOFTWARE DESCRIPTION

OVERVIEW

The three programs LAMCEL, LAMSUB and TRADYR constitute an analysis system for predicting the transient dynamic response of laminated composites, and in particular, the initiation of damage due to low velocity impact. The dynamic analysis utilizes the finite element method and consists of three stages; mass and stiffness characterization, numerical integration of the equations of motion, and postprocessing for stresses and strains. Either LAMCEL or LAMSUB may be used for the first and third stages, and TRADYR is used for the second.

LAMCEL is used to model laminated beams in two-dimensions, or rectangular plates in three. This program exploits the regular geometry of the uniform beam or rectangular plate to optimize the generation of the mass and stiffness of the structure. The dynamic properties of a representative 'cell' are generated by LAMCEL, and used to define the properties of the entire beam or plate in TRADYR.

LAMSUB may only be used to model three-dimensional plates, but is not restricted to rectangular geometries. This program generates the mass and stiffness matrices for any arbitrary sub-region of the plate.

TRADYR combines the mass and stiffness matrices generated by LAMCEL or LAMSUB to produce the mass and stiffness matrix for the beam or plate to be analyzed. To this it adds the dynamic properties of the impactor resulting in the equations of motion for the complete plate/impactor system. These equations of motion are then integrated numerically for the displacement history of the system.

The displacement history generated by TRADYR is used by either LAMCEL or LAMSUB to calculate the stress and strain histories of the structure. A failure analysis is also performed by these post processors to determine the onset of damage. It is assumed that the plate behaves as a linear elastic structure up to the initiation of damage with all nonlinearities being included in the contact model.

ANALYSIS PROCEDURE

Extensive use of substructuring is used in the analysis, resulting in models that include adequate detail without being prohibitively large. With this technique a small portion of the structure (substructure) is modeled in great detail with a large number of degrees of freedom. The equations of motion for this substructure are then reduced to include a much smaller number of 'master' degrees of freedom. All other degrees of freedom (slaves) will be expressed in terms of the masters.

Several substructures may then be combined to provide a coarse model for the dynamic analysis. By retaining all degrees of freedom along the boundaries between substructures as masters, a model having displacement compatability will be preserved. A further reduction in the assembled dynamic model is achieved by selecting a number of 'governor' degrees of freedom from the masters. The model is then condensed by defining the remaining master degrees of freedom in terms of the governors.

In a uniform beam or rectangular plate model, the structure may be divided into a number of uniform rectangular cells. These cells are identical, allowing the stiffness and inertial properties of a single cell to be generated once and used for all. For plates of arbitrary geometry, definition of a single representative cell may not be possible. These plates must be modeled using a number of unique substructures.

To complete the impact model a lumped mass representing the impactor is tied to a governor degree of freedom on the plate throught a non-conservative, non-linear spring. The plate then sees the impactor as simply a time varying force. The magnitude of the force and the amount of energy dissipated being functions of the relative motion between the plate and impactor.

The equations of motion for the resulting dynamic system are integrated to yield displacements, velocities and accelerations as functions of time. The integration is performed numerically, and displacement histories are stored on disk for subsequent post-processing. A restart capability is included in the numerical integration routine, allowing the analysis to be stoped, results reviewed, and the analysis restarted.

Displacement solutions predicted by the reduced dynamic model may be used to define the boundary conditions for refined stress analyses of the

original substructures. The substructure concept allows the stress analysis to be performed only for the regions of interest, such as in the vicinity of the impactor. To further minimize the computational effort, elements within a given substructure are specified for subsequent post processing. Stresses and strains are only calculated for those elements which have been specified.

Quantities which may be calculated for each element are stresses and strains in global and/or material coordinates. Global strains are calculated first and transformed into material coordinates for subsequent calculations. Stresses and strains are volume averaged over each ply within an element, and area averaged over interfaces. Unique interface properties may be defined for stress calculation purposes. The interface is assumed to have no volume and, therefore, does not contribute to the stiffness of the element.

A failure analysis is performed for each ply in each selected element, and for each interface. The model does not modify the stiffness of the structure, based on the prediction of failure, and may not be valid for analysis past the point of initial damage.

ELEMENT DESCRIPTION

Two- or three-dimensional solid finite elements are used to define the mass and stiffness matrices of the beam or plate respectively. The geometry of the two-dimensional element is defined by four corner nodes (Figure A1), and the three-dimensional element by eight corner nodes (Figures A2 and A3). Elements are allowed to have more than one ply throught the thickness but must contain complete plies.

Nodal variables for these elements consist of translations in each coordinate direction and the partial derivative of each translation with respect to each coordinate. This results in six degrees of freedom per node for the two-dimensional element, and twelve for the three-dimensional element. Cubic polynomials are used as shape functions to define the translational displacement fields for these elements.

Throughout this program, nodal degrees of freedom are referred to by the nomenclature Unm, where n is an integer from 1 to 3, and m is an integer from 0 to 3. Unm is then interpreted as the partial derivative of the

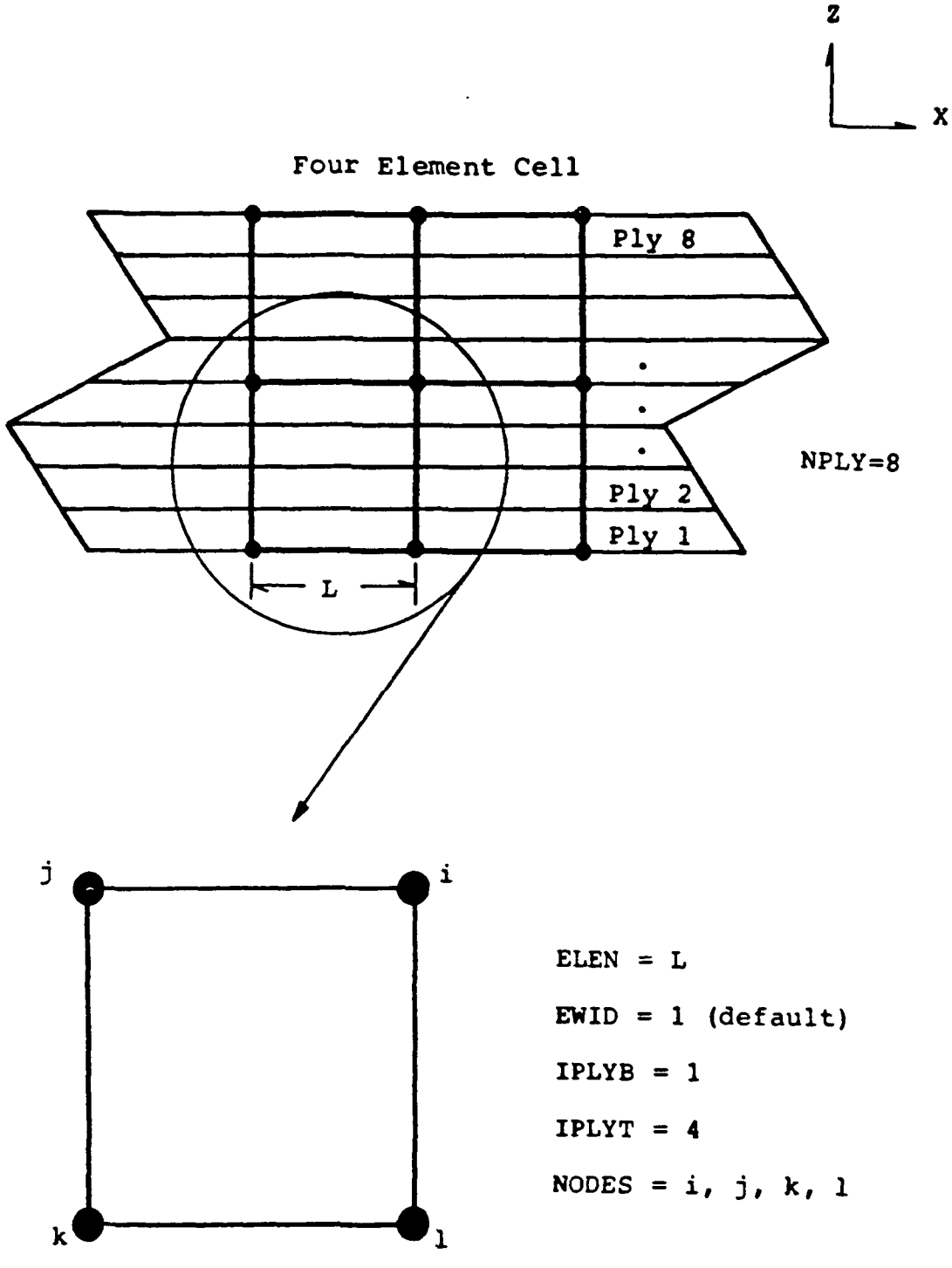

Figure A-1. 2-D Element Description

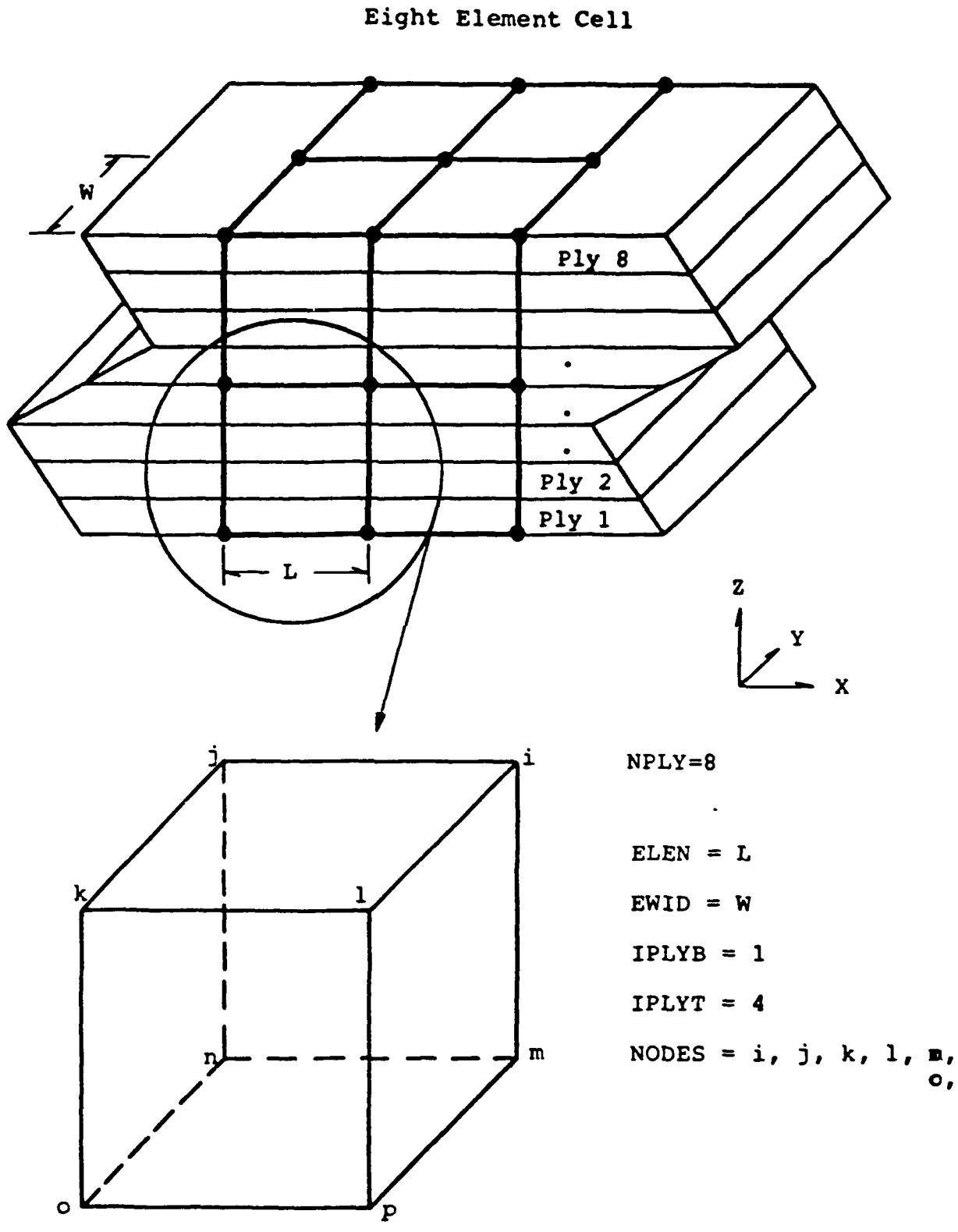

Figure A-2. 3-D Rectangular Element Description

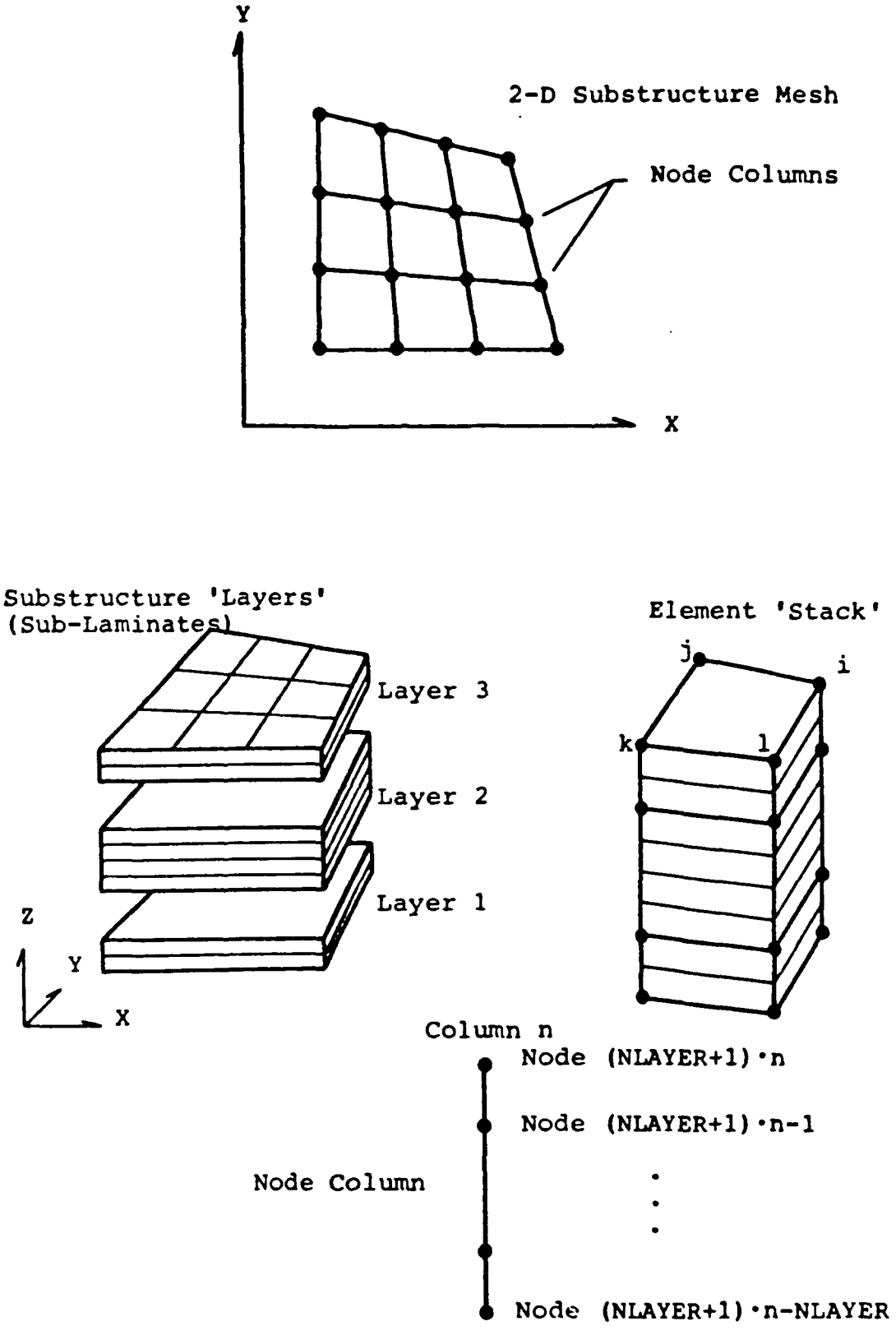

Figure A-3. 3-D General Element Description

translation in the n direction, with respect to the m coordinate. The only exception is when m is 0. For this case, Un0 is interpreted as the translation in the n direction. Relative to displacements, direction 1 is the global X direction, 2 is Y and 3 is Z, where the X, Y and Z axes form a right handed coordinate system. The Z direction is always assumed to be through the thickness of the laminate, and two-dimensional models are always defined in the X-Z plane.

Consistent mass matrices are generated using linear 'Serindipity' shape functions. The resulting matrix only associates mass with translational degrees of freedom. The algorithm used to numerically integrate the equations of motion requires that the reduced mass matrix be invertable. Since there is no mass associated with degrees of freedom other than translations, the reduced mass matrix for a system which included partial derivatives as governor degrees of freedom would have zeros on the diagonal. Such a matrix would not be invertable, disallowing the inclusion of partial derivatives as governor degrees of freedom.

LAMCEL AND LAMSUB - PROGRAM DESCRIPTIONS AND INPUT FORMAT

The programs LAMCEL and LAMSUB are similar in that both are used to generate the mass and stiffness matrices for a sub-region of a plate, and to perform stress analyses for those same sub-regions. Except for the definition of the finite element mesh used by each program, and minor differences in the control parameters, data input to the two programs is identical.

LAMCEL is used to generate the mass and stiffness matrices for a three-dimensional cell that is representative of the mass and stiffness of a small region of a rectangular plate. In addition, LAMCEL may be used to define a two-dimensional cell for analyzing the impact response of a uniform beam. Two-dimensional cells may assume states of either plane stress, or plane strain.

LAMSUB can only be used to analyze plates in three-dimensions but places no restriction on the geometry of the plate. The penalty paid for this increased flexiblility is increased run time, and more involved model definition.

For generation analyses, both programs read all input from an ASCII file named FILE01.DAT. Output is written to an ASCII file named FILE02.DAT, and a number of binary files named by the user. These binary files are used in subsequent dynamic analyses by TRADYR, and back substitution analyses by either LAMCEL or LAMSUB, as shown in Figures A-4 and A-5.

Back substitution analyses also require input from FILE01.DAT, and write to FILE02.DAT. In addition, a binary input file containing the displacement history predicted by TRADYR must also be furnished. The binary files written during the cell generation pass are also utilized during back substitution.

Data is read sequentially from FILE01.DAT with commas separating data items within a line of input. Successive commas will be interpreted as 0 or 0.0 for integer or real input. Detailed descriptions of the input data are included in the following sections.

A. Control

TITLE	78 character alphanumeric title.
NCHECK,NATYPE,NORDER,IMPRNT	The data check flag, analysis type flag, numerical integration order, and the expanded material property printout flag.

NCHECK = 0 (default), data check only.
= 1, analysis

In LAMCEL, NATYPE = 0, back substitution.
= 1, plane stress generation.
= 2, plane strain generation.
= 3, 3-D generation.

In LAMSUB, NATYPE = 0, back substitution.
= 1, 3-D generation.

$2 < NORDER < 4$

IMPRNT = 0 (default), print matrices.
= 1, do not print matrices.

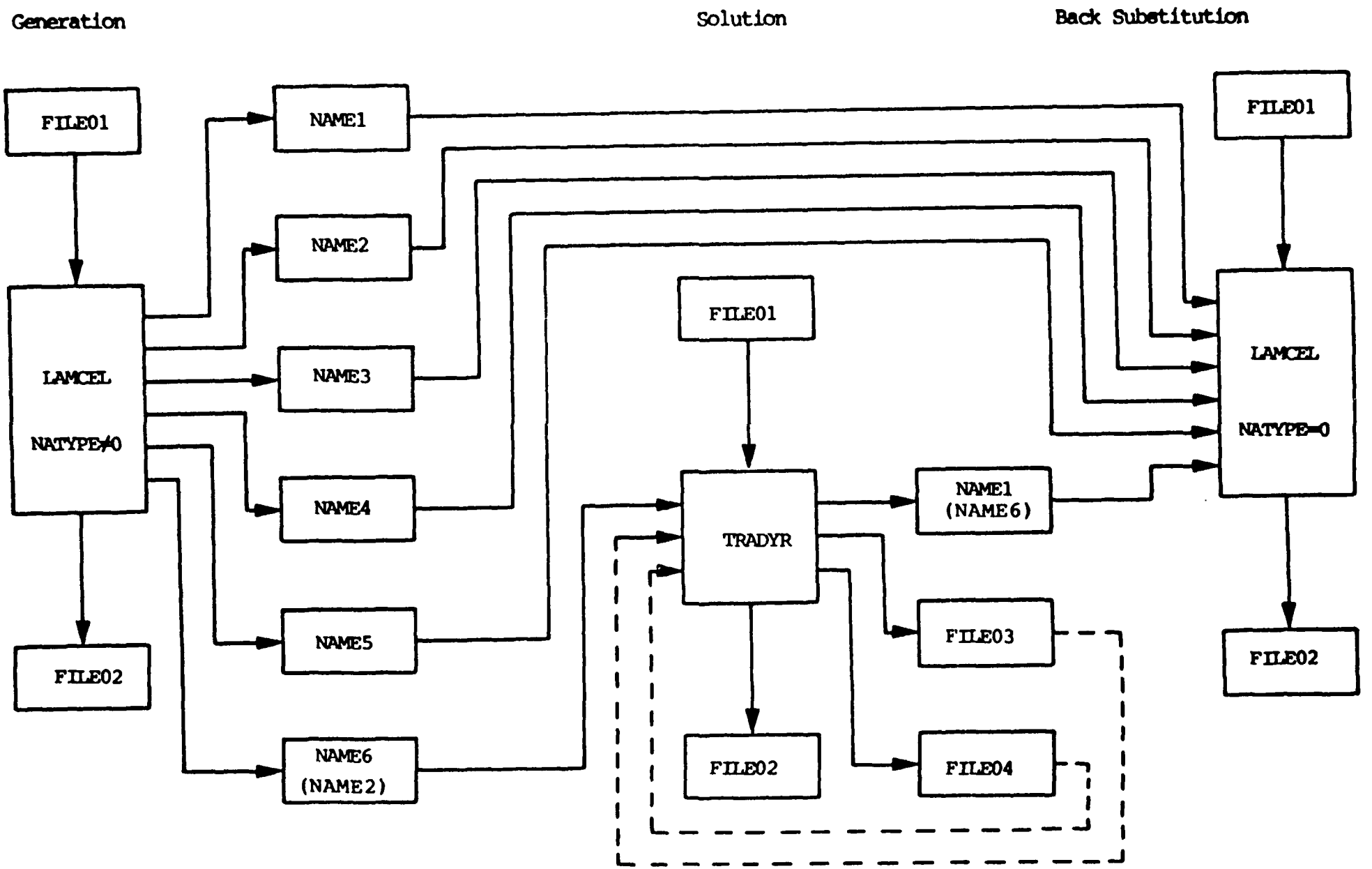

Figure A-4. LAMCEL File Usage

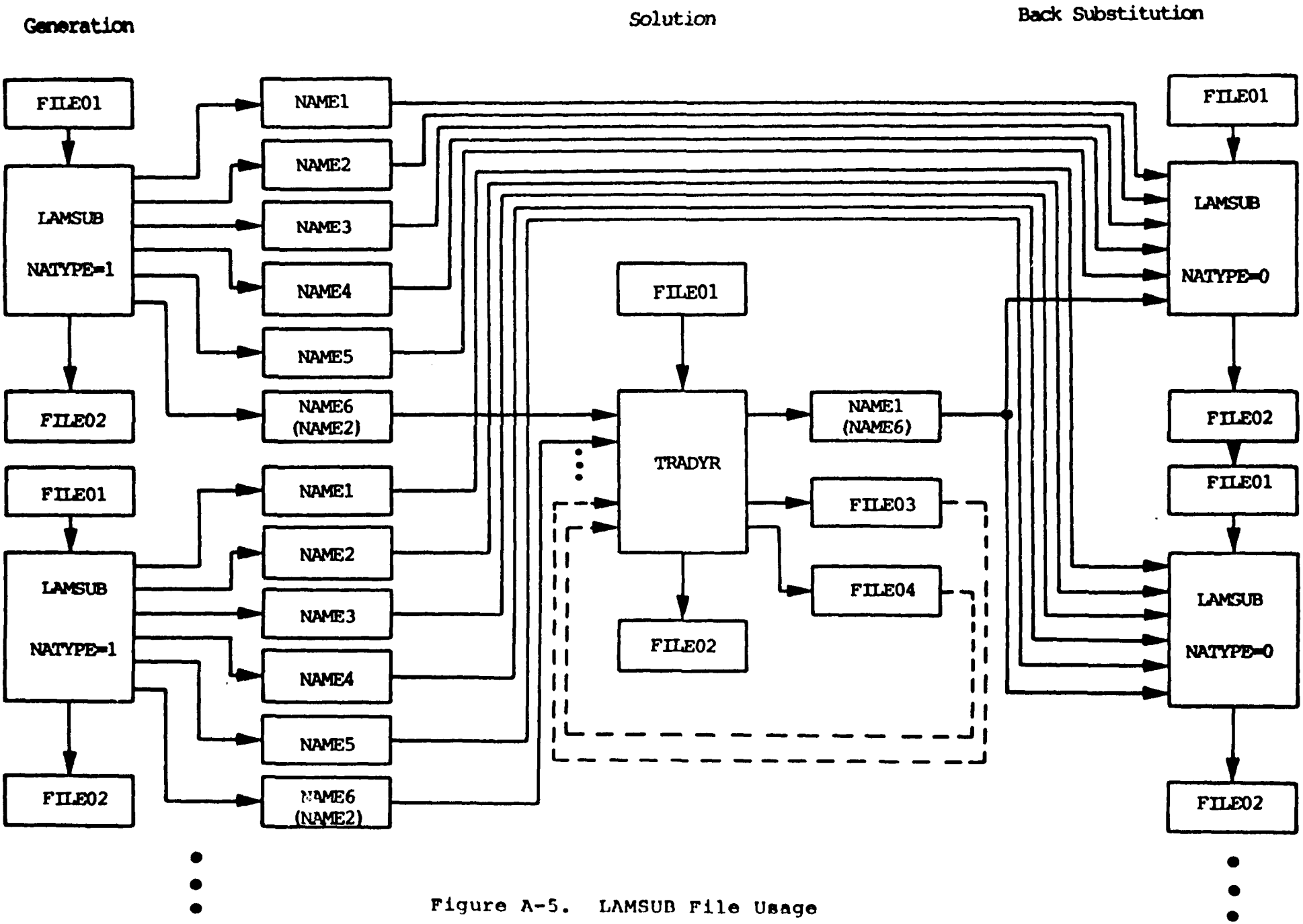

Figure A-5. LAMSUB File Usage

NAME1	Back substitution data storage file name. (40 character maximum)
NAME2	Lamina definition storage file name. (40 character maximum)
NAME3	Element definition storage file name. (40 character maximum)
NAME4	Constraint definition storage file name. (40 character maximum)
NAME5	Strain recovery data storage file name. (40 character maximum)
NAME6	If NATYPE > 0, constrained, condensed cell mass and stiffness matrix storage file name. If NATYPE = 0, displacement vector storage file name. (40 character maximum)

The program will branch at this point depending upon the value of NATYPE. If NATYPE is set to zero, the program will expect back substitution (Section B) information next. If NATYPE is set to any other valid value it will branch to the laminate description section (Section C).

NORDER specifies the order of the numerical integration algorithm used to calculate the stiffness matrices of elements. Two, three or four point integration may be specified. Expanded material property printout consists of the stress-strain matrix for each material in material coordinates, and the stress-strain matrix for each lamina in global coordinates. For back substitution analyses (NATYPE=0), NORDER and IMPRNT are not needed.

B. Back Substitution Information

NDISP,NSUBS — The index number of the displacement set to be used, and the index number of the substructure (cell) to be analyzed.

IDPRNT,(NPRINT(I),I=1,7) — The expanded displacement vector printout flag and the stress and strain printout flags. When a flag is set to 0 (default), the associated data set will be printed, if set to 1, the data will not be printed.

- IDPRNT - displacement vector.
- NPRINT(1) - global stresses.
- NPRINT(2) - global strains.
- NPRINT(3) - local stresses.
- NPRINT(4) - local strains.
- NPRINT(5) - ply printout.
- NPRINT(6) - interface printout.
- NPRINT(7) - surface printout.

NEBS — The number of elements for which stresses and strains will be calculated. The program will look for NEBS element numbers following this entry.

IELEM — The index number of the element for which stresses and strains will be calculated.

After performing a stress analysis on the last element specified in this set, the program will loop back to input the next values for NDISP and NSUBS. This loop will continue until an end of file is encountered while trying to read NDISP.

The files specified by NAME1 through NAME5 in the control section for a back substitution analysis must be the same as those defined in the generation analysis. The file specified by NAME6 is the same as that defined by NAME1 in TRADYR (see Figures A-4 and A-5). This file contains the displacement vector for each substructure in the assembled model at each print step. NDISP is the number of the print step for which the back substitution is being performed, and NSUBS is the index number of the substructure being analyzed.

Stresses and/or strains may be calculated in global and/or local coordinates. The quantities may be calculated at any or all of three locations; volume averages within plies, area averages of ply interfaces, and area averages at the surfaces of the laminate. The quantities calculated, and the locations at which they are calculated, are controlled by the flags NPRINT(2) through NPRINT(7).

C. Laminate Description

NMAT	The number of materials used in the laminate. The program will look for NMAT sets of material property input following this entry.
LABEL	40 character alphanumeric material label.
E1,E2,NU12,NU23,G12,RHO	Elastic constants for this material.
S1T,S1C,S2T,S2C,S12,S23	Strengths for this material.

NPLY,IFMAT	The number of plies in the laminate, and the index number of the material to be used for calculating interface stresses and strains. The program will look for NPLY lamina definitions following this entry.
MAT,T,THETA	The material index number, thickness and orientation of the ply.

Material property sets are assigned sequential index numbers based on the order in which they are input. Each set defines the properties for a unidirectional composite material for subsequent use in defining a particular laminate. Elastic constants E1 and E2 are the axial and transverse elastic moduli, NU12 and NU23 are the major Possion's ratios in the 1-2 and 2-3 planes, G12 is the shear mudulus in the 1-2 plane, and RHO is the density in mass density units. All other elastic constants are calculated assuming that the material is transversely isotropic.

Strengths S1T and S1C are the tensile and compressive axial strengths, S2T and S2C are the tensile and compressive transverse strengths, and S12 and S23 are the shear strengths in the 1-2 and 2-3 planes. As with elastic constants all other strengths are assigned assuming that the material is transversely isotropic in strength.

The laminate is defined by specifying the type of material and orientation of each ply starting at the bottom of the laminate and working up. Index numbers are assigned to the lamina sequentially based on the order in which they are input. The index numbers are subsequently used to specify which lamina are contained in a given element. The lamina definition parameter MAT specifies which set of material properties to use for a given lamina by referencing that materials index number. The parameter THETA specifies the rotation of the material 1 axis in the global X-Y plane. THETA is measured from the global X axis to the material 1 axis, in degrees, positive by the right hand rule.

All interfaces are assumed to have the same elastic properties and strengths. The properties specified by the parameter IFMAT are only used for stress and strain calculations, and do not contribute to the stiffness of the laminate.

Following the laminate description input, the program will look for cell (Section D.1) or substructure (Section D.2) definition input, depending upon which program is being run.

D.1 LAMCEL Cell Definition

NE	The number of elements in the cell. The program will look for NE sets of element definition input following this entry.
ELEN,EWID,IPLYB,IPLYT	The length and width of the element, and the index numbers of the bottom and top plies in the element.
(NODE(I),I=1,NNE)	The index numbers for the corners of the element. If NATYPE = 1 or 2, NNE = 4 = 3, NNE = 8

A cell is a refined finite element model of a small rectangular region of a laminate. Each element in the cell is assumed to be rectangular, and is defined by a length (ELEN) and width (EWID) in the X-Y plane, and the plies through its thickness (IPLYB and IPLYT). The thickness of an element is defined by the sum of the thicknesses of the plies contained in it, and is never specified explicitly. For two-dimensional analyses (NATYPE = 1 or 2), EWID may be omitted, and will default to 1.

Node positions are not specified explicitly, but are defined by the element geometries and connectivity. Element node numbers must be input in the order show in Figure A-1 for two-dimensional analyses, and Figure A-2 for three-dimensional analyses.

Elements are assigned sequential index numbers based on the order in which they are input. These index numbers serve as a means for referencing a particular element in subsequent post processing. The program will expect constraining information (Section E) following the cell definition input.

D.2 LAMSUB Substructure Definition

NLAYER	The number of layers of elements through the thickness of the laminate. The program will look for NLAYER layer definitions following this entry.
IPLYB,IPLYT	Index numbers for the bottom and top plies in the layer.
NC	The number of columns of nodes to be defined. The program will look for NC column definitions following this entry.
NCOL,X,Y,BETA	The index number of the column, its X and Y position, and the rotation of the nodal coordinate system relative to the global axes. Beta is input in degrees.
NS	The number of element stacks to be defined. The program will look for NS stack definitions following this entry.
NCOL(I),I=1,4	The node columns defining the corners of this stack.

The finite element mesh for the three-dimensional substructure is defined by a two-dimensional mesh of quadrilaterals in the X-Y plane, and information about the number and thickness of elements through the thickness of the laminate. Each of the quadrilaterals represents a stack of NLAYER elements having uniform geometry in the Z direction. The corners of the quadrilateral represent the position of a column of nodes which all have the same X and Y coordinates but different Z positions.

Each layer consists of one or more unidirectional plies and represents a one element thick mesh in the X-Y plane. The thickness of a layer is defined by the sum of the thicknesses of the plies contained in it, and is never specified explicitly. Layer interfaces and ply interfaces must not be confused. Layer interfaces must occur at ply interfaces, but ply interfaces do not necessarily have to be layer interfaces. The bottom most ply in the first layer must be ply 1 (IPLYB(1)=1), and subsequent layers must be input in order of increasing ply index. The index number of the bottom ply of layer n (IPLYB(n)) must be one greater than the index number of the top ply of layer n-1 (IPLYT(n-1)).

The program automatically places nodes through the thickness of the laminate for each location at which a nodal column in defined. The first of these nodes is placed at the bottom of the first layer; nodes are then located at each layer interface, starting with the bottom layer and working toward the top; the last node in the column is placed at the top of the last layer. Each column then consists of NLAYER+1 nodes. Each node is assigned a unique index number, based on the index number of the column it is located in. The index number of the first node in column n is given by (NLAYER+1)*(n-1)+1. Index numbers for subsequent nodes in that column are then incremented by 1.

The shape of an element stack may be any arbitrary quadrilateral, in the X-Y plane, and is uniform in the Z direction. The edges of the stack are defined by the index numbers of the four node columns at the corners of the quadrilateral. The order in which these indices are input must follow the convention shown in Figure A-3. Each stack consists of NLAYER elements through the thickness of the laminate. Elements are assigned sequential index numbers based on the order in which the stacks are input. Within a stack the element numbering begins with the bottom layer, incrementing by 1 as the top layer is approached. The index number for the nth element

(layer) in the mth stack of a laminate with NLAYER layers is given by NLAYER*(m-1)+n. These index numbers serve as a means for referencing a particular element in subsequent post processing.

The program will expect constraint information (Section E) following the cell definition input.

E. Constraints

NZDF	The number of constrained (fixed) displacements. The program will look for NZDF constraint definitions following this entry.
NODE,DIR	The node which is constrained, and the direction in which it is constrained.
NCS	The number of coupled sets. the program will look for NCS sets of coupled set input following this entry.
NIS,DIR	The number of nodes in the set, and the direction in which they are coupled.
NODE(I),I-1,NIS	Index numbers of the coupled nodes, input in groups of 10 per line.
NCE	The number of constraint equations. The program will look for NCE sets of constraint equation input following this entry.

NTE	The number of terms in the equation. The program will look for NTE constraint equation terms following this entry.
NODE,DIR,VALUE	Constraint equation term.

Three types of constraints may be defined for a given degree of freedom. The degree of freedom may be specified as having zero magnitude, the same magnitude as a similar degree of freedom, or a magnitude defined by a linear combination of several other degrees of freedom. These types of constraints are referred to as fixed displacements, coupled sets, and constraint equations, respectively.

The constraint definition NODE,DIR specifies that there will be no motion of at node NODE in the DIR direction. This degree of freedom is then removed from the problem and may not be used in any subseqent constraint definition or master degree of freedom specifications. If NODE is input as zero, all nodes will be constrained in the DIR direction.

Coupled sets force all of the specified nodes to have the same motion in the direction specified by DIR. The first node specified in the set remains active in that direction. For all other nodes in the set, that degree of freedom will be constrained out of the problem and may not be used in subsequent constraint definitions or master degree of freedom specifications.

Constraint equations are linear equations which define the motion of one degree of freedom in terms of one or more other degrees of freedom. The terms in the constraint equation input set are interpreted as

```
VALUE(1)*[NODE(1),DIR(1)] = VALUE(2)*[NODE(2),DIR(2)]
                          + VALUE(3)*[NODE(3),DIR(3)]
                          .
                          .
                          .
                          + VALUE(NTE)*[NODE(NTE),DIR(NTE)]
```

where [NODE(I),DIR(I)] specify the degree of freedom associated with the Ith term, and VALUE(I) is the coefficient multiplying that term. The degree of freedom specified in the first term of the set is constrained out of the problem, and may not be used in subsequent constraint definitions or master degree of freedom specifications.

Direction specifications (DIR) are three character labels of the form Unm, where n is an integer from 1 to 3, and m is an integer from 0 to 3. When m is zero, Un0 is interpreted as the translation in the n direction. When m is not zero, Unm is interpreted as the partial derivative of the translation in the n direction with respect to the m coordinate. For LAMCEL analyses, direction 1 is the global X direction, 2 is Y, and 3 is Z. For LAMSUB analyses, the nodal coordinate system (1,2,3) may be rotated relative to the global axes (X,Y,Z). Constraints are always specified in the nodal coordinate system. Directions 1 and 3 are the only valid directions for two-dimensional LAMCEL analyses.

When a model is generated that does not utilize a particular type of constraint the parameter which defines the number of sets of data for that type of constraint (NZDF, NCS or NCE) must still be included as zero. Following the constraint input, the program will look for master degree of freedom specifications (Section F).

F. Master Degrees of Freedom

NMDF	The number of master degrees of freedom. The program will look for NMDF master degree of freedom specifications following this entry.
NODE,DIR	The node number and direction that define the master degree of freedom.

Master degrees of freedom are assigned index numbers sequentially based on the order in which they are input. The first definition input will become master d.o.f. 1 of the cell regardless of the values of NODE and DIR;

the second will become master d.o.f. 2, and so on. Rows and columns of the constrained, condensed mass, and stiffness matrices for the cell will be arranged to reflect this numbering system.

The direction parameter DIR may be any valid label as defined in the constraint section (Section E). In addition, DIR may be assigned the label ALL, in which case all unconstrained degrees of freedom at the specified node will we retained as master degrees of freedom. If NODE is input as zero, the DIR degree of freedom at all nodes not constrained in the DIR direction will be retained as masters.

Master degree of freedom definitions are the last input data required by the program. After reading in this data set the program will print a cross reference of degree of freedom index numbers along with the total number of master, slave and constrained degrees of freedom. The mass and stiffness matrices are generated such that their rows and columns are arranged in the order specified by the cross reference.

TRADYR - PROGRAM DESCRIPTION AND INPUT FORMAT

TRADYR is a special purpose program that numerically integrates the equations of motion for a plate and impactor during a low velocity impact event. The program assembles the mass and stiffness matrices for the plate using the mass and stiffness matrices for cells or substructures generated by LAMCEL or LAMSUB. The equations of motion for the system are generated using these assembled matrices and the parameters which describe the impactor.

The complete set of simultaneous equations is reduced to a set of equations expressed in terms of a smaller number of 'governor' degrees of freedom which are defined by the user. The reduced equations of motion are then integrated numerically for the dynamic response of the system.

Input data is read from an ASCII file FILE01.DAT and from binary files written by LAMCEL or LAMSUB unless a restart analysis is being performed. For restart analyses input is read from FILE01.DAT and from the binary files FILE03.DAT and FILE04.DAT. These restart files are generated at the end of the original analysis and updated at the end of each restart analysis.

Output data is written to the ASCII file FILE02.DAT, and optionally, to a binary file specified by the user. The binary file contains the

displacement vector for each substructure at each print step. This file is necessary for subsequent post processing in either LAMCEL or LAMSUB.

Details of the required input data are given in the following sections.

A. Control

TITLE — 78 character alphanumeric title.

NCHECK,NRSTRT,NDOF — The data check flag, analysis restart flag and the number of degrees of freedom per node.

NCHECK = 0 (default), data check only.
= 1, analysis
NRSTRT = 0 (default), new analysis.
= 1, restart old analysis.
0 < NDOF < 13

INTALG,NTSTEP,NPRINT,NPSAVE — The numerical integration algorithm, the number of time steps, the number of time steps between solution printouts, and the solution save flag.

0 < INTALG < 5
NPSAVE = 0 (default), save solutions.
= 1, do not save solutions.

IDPRNT,IVPRNT,IAPRNT — The displacement, velocity and acceleration print flags.

IxPRNT = 0 (default), print solution
= 1, do not print solution

DELTA — The time increment.

NAME1	The name of the file in which the solutions will be stored. This entry is only included if NPSAVE = 0.

For restart analyses (NRSTRT = 1) no other input is required. However, the analysis restart files FILE03.DAT and FILE04.DAT written during the previous analysis must be provided. At the end of the analysis new restart files will be written over those originally provided. If the analysis is not a restart, the program will continue to look for input on FILE01.DAT. The parameter NDOF is not needed for restart analyses and will be ignored if included.

The program will perform NTSTEP time steps in the numerical integration of the equations of motion expanding and printing every NPRINT th step. A time step which will be expanded and printed is referred to as a print step. If NPSAVE has been set to zero, the displacement solution for every print step will be saved in binary on the file specified by the parameter NAME1. If NPSAVE has been set to 1, these solutions will not be saved and the parameter NAME1 is not input.

The amount of information printed at each print step depends upon the values of the print flags IDPRNT, IVPRNT, and IAPRNT. These flags correspond to the printing of the expanded displacement, velocity, and acceleration solutions respectively. When set to zero, the corresponding data set will be included in the printout. When set to 1, the data set will be omitted.

B. Model Definition

NE	The number of substructures in the model. The program will look for NE sets of substructure input after this entry.
NAME2	The name of the file from which the mass and stiffness matrices will be read.

NNE	The number of nodes in this substructure. The program will look for NNE node numbers following this entry, arranged in groups of ten per line.
(NODES(I),I=1,NNE)	The nodes defining this substructure.

The dynamic model consists of a number of substructures or cells for which the mass and stiffness have been previously defined and stored. This section of TRADYR assembles the mass and stiffness matrices for these substructures into a model of the complete structure. The degrees of freedom in this model are the master degrees of freedom for the individual substructures.

To ease the effort in defining the substructures (cells) that comprise a model, each substructure is assumed to be defined by a given number of nodes each having NDOF degrees of freedom. These degrees of freedom are the master degrees of freedom, specified for the substructure in either LAMCEL or LAMSUB. This method assumes that the same degrees of freedom were retained for all nodes at which masters were defined. If this is not the case NDOF should be set to 1 and each 'node' on the substructure is actually a degree of freedom.

LAMCEL and LAMSUB assign index numbers to master degrees of freedom based on the order in which they were input, and arrange the rows and columns of the reduced mass and stiffness matrices to reflect this order. The definition of the nodes which define the substructure in TRADYR must also use this same order.

C. Constraints

NZDF	The number of constrained (fixed) displacements. The program will look for NZDF constraint definitions following this entry.

NODE,DIR	The node which is constrained, and the direction in which it is constrained.
NCS	The number of coupled sets. the program will look for NCS sets of coupled set input following this entry.
NIS,DIR	The number of nodes in the set, and the direction in which they are coupled.
NODE(I),I=1,NIS	Index numbers of the coupled nodes, input in groups of 10 per line.
NCE	The number of constraint equations. The program will look for NCE sets of constraint equation input following this entry.
NTE	The number of terms in the equation. The program will look for NTE constraint equation terms following this entry.
NODE,DIR,VALUE	Constraint equation term.

Constraint definitions in TRADYR are interpreted in the same manner as constraint definitions in LAMCEL or LAMSUB. The user is referred to Section E of the LMACEL and LAMSUB program descriptions for details of these definitions. The only exception being the set of valid direction specification labels.

Direction specifications (DIR) are three character labels of the form Unm, where n and m are integers whose values depend upon the value of NDOF. If NDOF is six or twelve the direction convention defined in Section E for two- or three-dimensional analyses is maintained. If NDOF is any other value, nm is a two character integer ranging from 01 to 12. Only the first NDOF integers are valid labels, and a zero must preceed integers less than ten. Directions are always specified in nodal coordinates which may not be parallel to the global coordinates.

D. Governor Degrees of Freedom

NGDF	The number of governor degrees of freedom. The program will look for NGDF governor degree of freedom specifications following this entry.
NODE,DIR	The node number and direction that define the governor degree of freedom.

The direction parameter DIR may be any valid label as defined in the constraint section (Section C). In addition, DIR may be assigned the label ALL, in which case all unconstrained degrees of freedom at the specified node will we retained as governor degrees of freedom. If NODE is input as zero, the DIR degree of freedom at all nodes not constrained in the DIR direction will be retained as governors.

E. Impact Parameters

NODE,DIR	The node at which the impact occurs and the direction of the impact.
MIMP,K,N,M,I,C	The mass of the impactor and the five spring constants.

U0,V0	The initial position and velocity of the impactor.